The effects of continental margins and water mass circulation on the distribution of dissolved aluminum and manganese in Drake Passage

R. Middag,[1,2] H. J. W. de Baar,[1,3] P. Laan,[1] and O. Huhn[4]

Received 7 July 2011; revised 26 October 2011; accepted 22 November 2011; published 28 January 2012.

[1] A total of 232 samples were analyzed for concentrations of dissolved aluminum ([Al]) and manganese ([Mn]) in Drake Passage. Both [Al] and [Mn] were extremely low (~0.3 and 0.1 nM, respectively) in the surface layer of the middle Drake Passage, most likely due to limited input and biological uptake/scavenging. Elevated [Al] (>14 nM) and [Mn] (>2 nM) over the South American continental shelf are related to land run-off, whereas elevated concentrations (>1 nM and >2 nM, respectively) near the Antarctic Peninsula are most likely related to sediment re-suspension. Re-suspension of sedimentary particles and pore waters influences the distribution of [Al] and [Mn] over the continental slopes on both sides of Drake Passage. The influence of the continental margins and accumulated dust input potentially explains the higher [Al] observed eastward in the Atlantic section of the Southern Ocean. In the northern Drake Passage, elevated [Al] (~0.8 nM) and [Mn] (~0.3 nM) near the seafloor are most likely the result of bottom sediment re-suspension by the relatively strong currents. In the deep southern Drake Passage sediment re-suspension associated with the inflow of Weddell Sea Deep Water appears to cause elevated [Al] (>1 nM) and [Mn] (~0.4 nM). In the deep northern Drake Passage, North Atlantic Deep Water brings in elevated [Al] and Southeast Pacific Deep Slope Water brings in the signature of Pacific hydrothermal vents. Elevated [Mn] and δ^3He were correlated in this water layer and are most likely originating from the volcanically active ridges in the Pacific Ocean.

Citation: Middag, R., H. J. W. de Baar, P. Laan, and O. Huhn (2012), The effects of continental margins and water mass circulation on the distribution of dissolved aluminum and manganese in Drake Passage, *J. Geophys. Res.*, *117*, C01019, doi:10.1029/2011JC007434.

1. Introduction

[2] Drake Passage (Figure 1) is the narrowest passage for the Antarctic Circumpolar Current (ACC) and connects the Pacific and Atlantic Oceans. Drake Passage is about 800 km wide at its shortest crossing between Cape Horn (Chile) and Greenwich Island (South Shetland Islands). The hydrography of Drake Passage is reasonably well studied due to its important role in global ocean circulation. Much less is known however, about the trace metal distributions and biogeochemical cycles. The aim of this paper is to start filling in this void for dissolved aluminum (Al) and manganese (Mn). During the International Polar Year (2007–2008) an expedition aboard R/V *Polarstern* went to the Southern Ocean and crossed Drake Passage. The GEOTRACES team onboard sampled this understudied region over the entire water column.

[3] Dissolved Al occurs in a wide range of concentrations in the open ocean and the distribution of Al shows the strongest interbasin fractionation known for any trace metal [*Bruland and Lohan*, 2004]. In the central North Pacific concentrations are 8 to 40 times lower than at corresponding depth in the central North Atlantic [*Orians and Bruland*, 1985]. In the Arctic Ocean concentrations of dissolved Al ([Al]) have recently been shown to correlate with the concentrations of Si [*Middag et al.*, 2009] as has been reported before in the Mediterranean Sea [*Hydes et al.*, 1988; *Chou and Wollast*, 1997]. However, actual concentrations are very different as in the deep Mediterranean [Al] is up to 174 nM [*Hydes et al.*, 1988] while concentrations in the deep Arctic Ocean are only up to 28 nM [*Middag et al.*, 2009].

[4] The fractionation of dissolved Al between ocean basins is the result of differences in input and removal and the relative short residence time of Al compared to the ocean circulation [e.g., *Orians and Bruland*, 1985, 1986; *Measures and Edmond*, 1990; *Middag et al.*, 2011a; *Stoffyn and Mackenzie*, 1982]. In the surface ocean, the particle reactive Al has a short residence time of only ~10 days in coastal waters with high concentrations of lithogenic material

[1]Royal Netherlands Institute for Sea Research, Den Burg, Netherlands.
[2]Department of Ocean Sciences and Institute of Marine Sciences, University of California, Santa Cruz, California, USA.
[3]Department of Ocean Ecosystems, University of Groningen, Groningen, Netherlands.
[4]Institut für Umweltphysik, Universität Bremen, Bremen, Germany.

0148-0227/12/2011JC007434

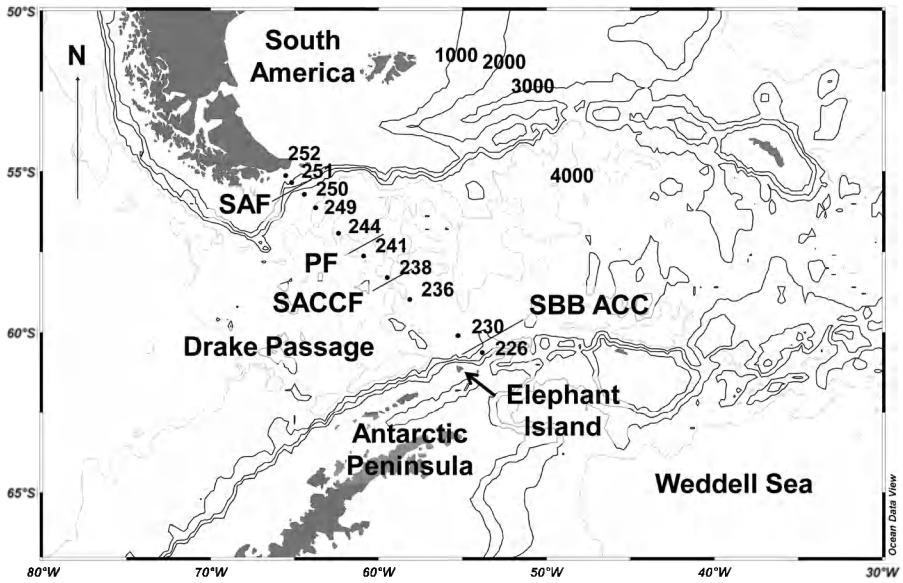

Figure 1. Trace metal sampling stations crossing Drake Passage during cruise ANT XXIV/3 from 1 to 16 April 2008 from just east of Elephant Island near the Antarctic Peninsula to the southeast tip of Tierra del Fuego (Argentina) aboard R/V *Polarstern*. Abbreviations in alphabetical order: PF: Polar Front; SACCF: Southern Antarctic Circumpolar Current Front; SAF: Sub-Antarctic Front; SB ACC: Southern Boundary of the Antarctic Circumpolar Current.

[*Brown et al.*, 2010] to 4 years [*Orians and Bruland*, 1986] in the oligotrophic open ocean. The removal of Al from the water column can be passive scavenging [e.g., *Hydes*, 1979; *Moore and Millward*, 1984; *Orians and Bruland*, 1985], but also active uptake of Al by diatoms [e.g., *Stoffyn*, 1979; *Gehlen et al.*, 2002, *Middag et al.*, 2009]. In the deep ocean the residence time of Al is much longer, between 50 and 200 years [*Orians and Bruland*, 1985, 1986], due to less scavenging. However, this relatively long deep ocean residence time is still much shorter than the time scale of ocean circulation and the deep ocean water mass renewal time of about 1000 years. Therefore deep [Al] depends on local sources like diffusion from sediments [*Hydes*, 1977], pressure dependent solubility of Al-containing particles [*Moore and Millward*, 1984] and deep convection [*Measures and Edmond*, 1992; *Middag et al.*, 2009]. Upwelled deep water is generally low in dissolved Al and extra Al can only be supplied to surface waters by external lithogenic sources, i.e., dissolution of aeolian dust input from above, river input or input from partial dissolution of lithogenic (shelf) sediments. Much of the river input of dissolved Al precipitates due to estuarine removal processes [*Mackin and Aller*, 1984a, 1984b] and does not reach the open ocean in significant quantities [*Tria et al.*, 2007, and references therein]. In the open ocean, the surface [Al] has been related to atmospheric dust input (initial model by *Measures and Brown* [1996]) which varies markedly between ocean regions [e.g., *Measures and Vink*, 2000; *Gehlen et al.*, 2003; *Kramer et al.*, 2004; *Han et al.*, 2008].

[5] Manganese (Mn) is an essential nutrient. Like Al, it exists in nanomolar concentrations in the world's oceans [e.g., *Elderfield*, 1976], despite the high abundances in the earth's crust [*Wedepohl*, 1995]. In natural seawater the distribution of Mn is largely controlled by redox chemistry. Dissolved Mn occurs as Mn ions, but these are thermodynamically unstable in the presence of oxygen and will tend to precipitate as insoluble Mn oxides [*Sunda and Huntsman*, 1994]. Mn oxides that form in oxic seawater are eventually lost from the water column by particulate scavenging and sinking. Microbial Mn oxidation promotes the removal of dissolved Mn from seawater [*Sunda and Huntsman*, 1988, and references therein; *Tebo et al.*, 2007, and references therein]. In the photic zone however, Mn can be reduced back to soluble Mn ions by photo reduction [*Sunda et al.*, 1983; *Sunda and Huntsman*, 1988, 1994]. This photo reduction in combination with other surface sources like atmospheric input [e.g., *Landing and Bruland*, 1980; *Baker et al.*, 2006] or fluvial input [e.g., *Elderfield*, 1976; *Aguilar-Islas and Bruland*, 2006; *Middag et al.*, 2011b] lead to the elevated surface concentrations of Mn typically observed in the open ocean. The algal community may remove Mn actively [*Sedwick et al.*, 1997], and recently a depletion of Mn in constant proportion to phosphate depletion has been observed in the surface waters of the Southern Ocean [*Middag et al.*, 2011c]. Below the surface layer and absent any sources of Mn, oxidative precipitation and subsequent loss of dissolved Mn from the water column lead to low background concentrations. These have been estimated to be around 0.15 nM in the deep Atlantic Ocean [*Statham et al.*, 1998] and similarly low deep concentrations have been reported for the Pacific Ocean [*Landing and Bruland*, 1980, 1987]. In the absence of oxygen the concentrations of dissolved Mn ([Mn]) are much higher, for example in the deep anoxic water column and sediments of the Black Sea or Cariaco Trench, concentrations as high as 8.1 μM have been observed [e.g., *Jacobs et al.*, 1987; *Haraldsson and Westerlund*, 1988; *Lewis and Landing*, 1991; *Yemenicioglu et al.*, 2006; *Percy et al.*, 2008].

[6] Other sources of Mn are hydrothermal input [*Klinkhammer et al.*, 1977; *Klinkhammer and Bender*, 1980] and dissolution from sediments, especially from continental

shelves with reducing sediments [*Heggie et al.*, 1987; *Laës et al.*, 2007]. Active hydrothermal vents are most prominent in fast spreading regions like the deep Pacific, but are also found in slower spreading regions [*Baker and German*, 2004]. Hydrothermal vents release high concentrations of reduced trace metals like Mn and iron (Fe), but also primordial trace gases like helium (He) [*Well et al.*, 2003; *Farley et al.*, 1995]. In the productive shelf seas, the export of particulate matter to the seafloor and the subsequent microbial breakdown with associated oxygen consumption can lead to anoxic or suboxic conditions in the sediment. Under these circumstances Mn gets mobilized from the sediments into the pore water [*Rutgers van der Loeff et al.*, 1990] and can subsequently diffuse into the overlying water column by a gradient flux [e.g., *Sundby and Silverberg*, 1985; *Pakhomova et al.*, 2007].

[7] Pore waters and partial dissolution of shelf sediments can be a source of trace metals in the ocean adjacent to the shelf, especially in a relatively narrow channel like Drake Passage. In the deep Drake Passage the waters of the ACC are influenced by both Pacific and Atlantic Ocean waters. Moreover, due to the close proximity of South America, dust input has to be considered as a surface source of Al and Mn for Drake Passage. Biological uptake of Mn is likely a sink for Mn, as low [Mn] in the surface layer of Drake Passage has been reported previously [*Martin et al.*, 1990]. The combination of these different processes affecting the distributions of Al and Mn in the relatively narrow region of Drake Passage, combined with low concentrations, make this one of the most challenging and therefore interesting ocean regions to assess and interpret the trace metal distributions.

2. Methods

[8] Samples were collected in April 2008 aboard R/V *Polarstern* during expedition ANT XXIV/3 departing 10 February from Cape Town (South Africa) and arriving 16 April at Punta Arenas (Chile). The transect crossing Drake Passage (Figure 1) from just east of Elephant Island near the Antarctic Peninsula to the southeast tip of Tierra del Fuego (Argentina) consisted of 10 Trace Metal (TM) stations, each comprising 24 sampling depths. At TM stations seawater was collected using 24 internally Teflon-coated PVC 12 L GO-FLO samplers (General Oceanics, Inc.) mounted on an all-titanium frame which was connected to a Kevlar wire and controlled from onboard [*de Baar et al.*, 2008]. These GO-FLO's were conditioned (not acid or detergent washed) at the beginning of the cruise by lowering and again recovering the open samplers throughout the full ~4km depth of the open ocean water column.

[9] Samples for Al and Mn analysis were collected from the GO-FLO bottles in a class 100 clean room environment [*de Baar et al.*, 2008]. The water was filtered directly from the GO-FLO sampler through a 0.2 μm filter capsule (Sartrobran-300, Sartorius) under nitrogen pressure (1.5 atm). Therefore all trace metal data reported in this paper is categorized dissolved. The Low Density Polyethylene bottles (LDPE, Nalgene) used for the storage of reagents and samples were cleaned according to an intensive three step cleaning procedure as described by *Middag et al.* [2009]. Filtered seawater samples were taken in cleaned LDPE sample bottles (125 ml) from each GO-FLO sampler. All sample bottles were rinsed five times with the sample seawater.

[10] Due to the water requirement of other cruise participants 232 samples (instead of 240 samples) were analyzed for Al and Mn from the 10 deployments at the TM stations. Of the 232 samples analyzed, 18 samples (7.8%) for Al and 11 samples (4.7%) for Mn were suspected outliers and therefore not further used in data analysis and figures presented here. Suspected outliers were identified following criteria as described by *Middag et al.* [2011a, 2011c]. The complete relational database includes specific flags for suspect or rejected outlier values and will be available at the international GEOTRACES datacenter (http://www.bodc.ac.uk/geotraces/) and can also be found in the auxiliary material.[1]

[11] Analysis of dissolved Al was performed onboard as described by *Middag et al.* [2011a] with the lumogallion fluorometric method (flow injection) after *Brown and Bruland* [2008]. The system was calibrated for every station using standard additions to filtered acidified seawater with a low concentration of Al that was collected in the region. The blank was determined for every station and the average blank value was 0.17 nM (SD = 0.02 nM; n = 10). The value of 0.2 nM was the maximum allowed blank before starting a series of analyses. The limit of detection, defined as three times the standard deviation of the lowest concentration observed, was 0.07 nM. An internal reference sample was analyzed 36 times on different days during the entire cruise (average 3.56 nM) and the relative standard deviation of the 36 analyses was 3.16%. The relative standard deviation of the triplicate analyses on the separate days was on average 1.5%. The flow injection system was cleaned every day by rinsing with a 0.5 M HCl solution. Samples of the SAFe intercalibration program [*Johnson et al.*, 2007] were analyzed in triplicate. Results for both SAFe Surface (S; 1.68 $\pm$ 0.04 nM; n = 8) and SAFe deep (D2; 1.01 $\pm$ 0.08 nM; n = 17) from 1000 m water are in good agreement [*Middag et al.*, 2011a] with the community consensus values (S; 1.74 $\pm$ 0.09 nM and D2; 1.04 $\pm$ 0.10 nM, http://www.geotraces.org/).

[12] Analysis of dissolved Mn was performed onboard as described by *Middag et al.* [2011c] with the luminol chemiluminescence flow injection analysis method developed by *Doi et al.* [2004], modified to buffer the samples in-line [*Middag et al.*, 2011c]. The system was calibrated for every station using standard additions to filtered acidified seawater with a low concentration of Mn that was collected in the region. The blank was determined for every station and the average blank value was 0.02 nM (SD = 0.003 nM, n = 10). The limit of detection defined as three times the standard deviation of the blank was <0.01 nM. An internal reference sample was analyzed 40 times on different days during the entire cruise (average 0.44 nM) and the relative standard deviation of the 40 analyses was 3.2%. The relative standard deviation of the triplicate analyses on the separate days was on average 1.3%. The flow injection system was rinsed every day with a 0.5 M HCl solution. Samples of the SAFe intercalibration program [*Johnson et al.*, 2007] were analyzed in triplicate. The resulting concentrations of Mn for both SAFe Surface (S) (0.73 nM, n = 1) and SAFe deep (D2) from

[1]Auxiliary materials are available at ftp://ftp.agu.org/apend/jc/2011jc007434.

Table 1. Station and Hydrocast Number, Date, Position and Water Column Depth of 10 TM Stations and 22 Regular CTD/Rosette Hydrocasts in Drake Passage

Station/Cast	Date	Latitude	Longitude	Depth (m)	TM/Regular
PS71/225-1	01.04.08	60° 42.49′ S	53° 36.93′ W	1463.2	Regular
PS71/226-2	01.04.08	60° 37.61′ S	53° 49.75′ W	2775.0	TM
PS71/227-1	02.04.08	60° 32.04′ S	54° 5.41′ W	2977.7	Regular
PS71/228-1	02.04.08	60° 26.71′ S	54° 19.12′ W	3177.7	Regular
PS71/229-1	02.04.08	60° 16.19′ S	54° 47.79′ W	3268.5	Regular
PS71/230-6	03.04.08	60° 6.12′ S	55° 16.35′ W	3515.2	TM
PS71/231-2	03.04.08	59° 54.95′ S	55° 44.76′ W	3575.7	Regular
PS71/232-1	03.04.08	59° 45.02′ S	56° 14.20′ W	3636.2	Regular
PS71/233-2	04.04.08	59° 33.50′ S	56° 39.91′ W	3579.5	Regular
PS71/234-1	05.04.08	59° 21.47′ S	57° 8.61′ W	3557.2	Regular
PS71/235-1	05.04.08	59° 9.42′ S	57° 37.90′ W	3647.5	Regular
PS71/236-3	05.04.08	58° 58.23′ S	58° 8.32′ W	3787.7	TM
PS71/237-1	06.04.08	58° 39.20′ S	58° 47.45′ W	3933.7	Regular
PS71/238-2	06.04.08	58° 18.10′ S	59° 28.62′ W	3077.0	TM
PS71/239-1	07.04.08	58° 5.93′ S	60° 0.24′ W	4069.5	Regular
PS71/240-1	07.04.08	57° 52.55′ S	60° 27.94′ W	3986.5	Regular
PS71/241-6	07.04.08	57° 37.63′ S	60° 53.80′ W	3424.2	TM
PS71/242-1	08.04.08	57° 30.57′ S	61° 7.78′ W	3900.5	Regular
PS71/243-1	08.04.08	57° 24.38′ S	61° 24.12′ W	3739.2	Regular
PS71/244-3	08.04.08	56° 55.16′ S	62° 23.72′ W	4095.5	TM
PS71/246-1	09.04.08	57° 7.09′ S	61° 58.32′ W	3773.2	Regular
PS71/247-1	10.04.08	56° 40.17′ S	62° 49.13′ W	4069.2	Regular
PS71/248-1	10.04.08	56° 25.06′ S	63° 18.26′ W	3983.5	Regular
PS71/249-3	10.04.08	56° 7.16′ S	63° 45.44′ W	4302.0	TM
PS71/250-6	11.04.08	55° 42.06′ S	64° 25.67′ W	3798.0	TM
PS71/251-3	12.04.08	55° 20.01′ S	65° 10.68′ W	1631.0	TM
PS71/252-1	12.04.08	55° 7.70′ S	65° 32.00′ W	408.5	TM
PS71/253-1	12.04.08	55° 13.83′ S	65° 21.29′ W	1053.5	Regular
PS71/254-1	13.04.08	55° 28.21′ S	64° 57.20′ W	2576.7	Regular
PS71/255-1	13.04.08	55° 35.61′ S	64° 44.55′ W	3619.7	Regular
PS71/256-1	13.04.08	55° 53.33′ S	64° 15.52′ W	3877.2	Regular
PS71/258-1	13.04.08	56° 0.67′ S	64° 0.51′ W	3985.2	Regular

1000 m (0.32 ± 0.01 nM, n = 37) agree with the majority of the labs contributing to the consensus value (http://www.geotraces.org/science/intercalibration) [*Middag et al.*, 2011c].

[13] Regular CTD/Rosette hydrocasts were done in addition to the special TM hydrocasts (Table 1). These regular hydrocasts were done at separate stations and as additional hydrocasts at most TM stations, as not all samples could be taken from the all-titanium trace metal sampling system. The salinity (conductivity), temperature and depth (pressure) were measured with two different CTD's of same type (Seabird SBE 911+), one from the Netherlands Institute for Sea Research (NIOZ) mounted on the all-titanium trace metal sampling system for TM hydrocasts and one from the Alfred Wegener Institute (AWI) on the regular CTD/Rosette used for regular hydrocasts. Both had been calibrated before and after the expedition by the company (Seabird). Moreover, the conductivity sensors were calibrated during the cruise against salinity samples measured onboard. Light transmission was measured using a transmissometer (WET Labs C-Star SN CST-814DR) mounted on the regular CTD. Light transmission data was converted to coefficient of attenuation (= −ln (transmission)/(transmissometer path length)) which is linearly related to the amount of particles present in the water column.

[14] Samples for He isotopes were taken from the regular CTD/Rosette hydrocasts and not from the TM hydrocasts. The samples were drawn and stored in gas-tight copper tubes [*Sültenfuß et al.*, 2009] and later analyzed in the laboratory (IUP, Institute für Umweltphysik, Universität Bremen, Germany). The extracted gases from the seawater samples were analyzed with a mass spectrometer system as described by *Sültenfuß et al.* [2009]. The accuracy for the isotope ratio (δ^3He = 100 × ([^{3}He/^{4}He]$_{observed}$/[^{3}He/^{4}He]$_{atmosphere}$ − 1) in %) is 0.4%.

3. Hydrography

[15] Several fronts exist in the relatively narrow Drake Passage: in moving south from Chile the Sub-Antarctic Front (SAF), the Polar Front (PF), the Southern Antarctic Circumpolar Current Front (SACCF) and the Southern Boundary of the Antarctic Circumpolar Current Front (SB ACC). The latter is also known as the Continental Water Boundary or Southern Boundary (SBdy). South of the SAF the Antarctic Circumpolar Current (ACC) flows eastward, extending unbroken around the globe. Within the ACC the mentioned PF and SACCF are found (Figure 2).

[16] The SAF is defined as 'the location of the rapid descent of the salinity minimum' (looking from south to north) by *Whitworth and Nowlin* [1987] or by the maximum subsurface temperature gradient between the 4° and 5°C isotherms at 400 m depth [*Lenn et al.*, 2008]. According to these definitions the SAF is located between TM station 251 and regular station 254 (Figure 2; regular stations listed in Table 1). The PF is defined as the location where the temperature minimum begins its rapid descent to greater depth (looking from south to north) by *Whitworth and Nowlin* [1987] or as the northernmost extent of the 2°C subsurface temperature minimum by *Pollard et al.* [2002]. According to both definitions the PF was located between regular stations 242 and 243 (between TM stations 241 and 244). The zone between the SAF and the PF is known as the Polar Frontal Zone (PFZ). The SACCF is defined as location where the potential density anomaly (σ_θ) at 500 decibar (db) decreases below 27.70 kg·m^{-3} (looking from south to north) by *Barré et al.* [2008]. According to this definition the SACCF was located between regular station 237 and TM station 238. The SB ACC is defined as the maximal thermal gradient in the potential temperature (θ) maximum [*Klatt et al.*, 2005] or as the location where the σ_θ at 500 db decreases below 27.75 kg·m^{-3} (looking from south to north) by *Barré et al.* [2008]. According to both definitions the SB ACC was located between regular station 228 and 229 (between TM stations 230 and 236). The zone between the PF and the SB ACC is known as the Antarctic Zone (AAZ) and to the south of the SB ACC the Weddell Scotia Confluence Zone (WSCZ) is found.

[17] Along the transect several water masses can be distinguished [*Sudre et al.*, 2011], which are briefly summarized here. Water masses with typical potential temperatures are detailed in the legend of Figure 2. South of the SAF, Sub-Antarctic Surface Water (SSW) is found and south of the PF (AAZ) the cold and relatively fresh Antarctic Surface Water (AASW) constitutes the upper water layer.

[18] The core of Antarctic Intermediate Water (AAIW) is found around 1000 m depth close to the continental slope of South America and southwards (within the PFZ) the AAIW raises to about 500 m. Within the ACC (between the SAF and the SB ACC) the most extensive subsurface water mass

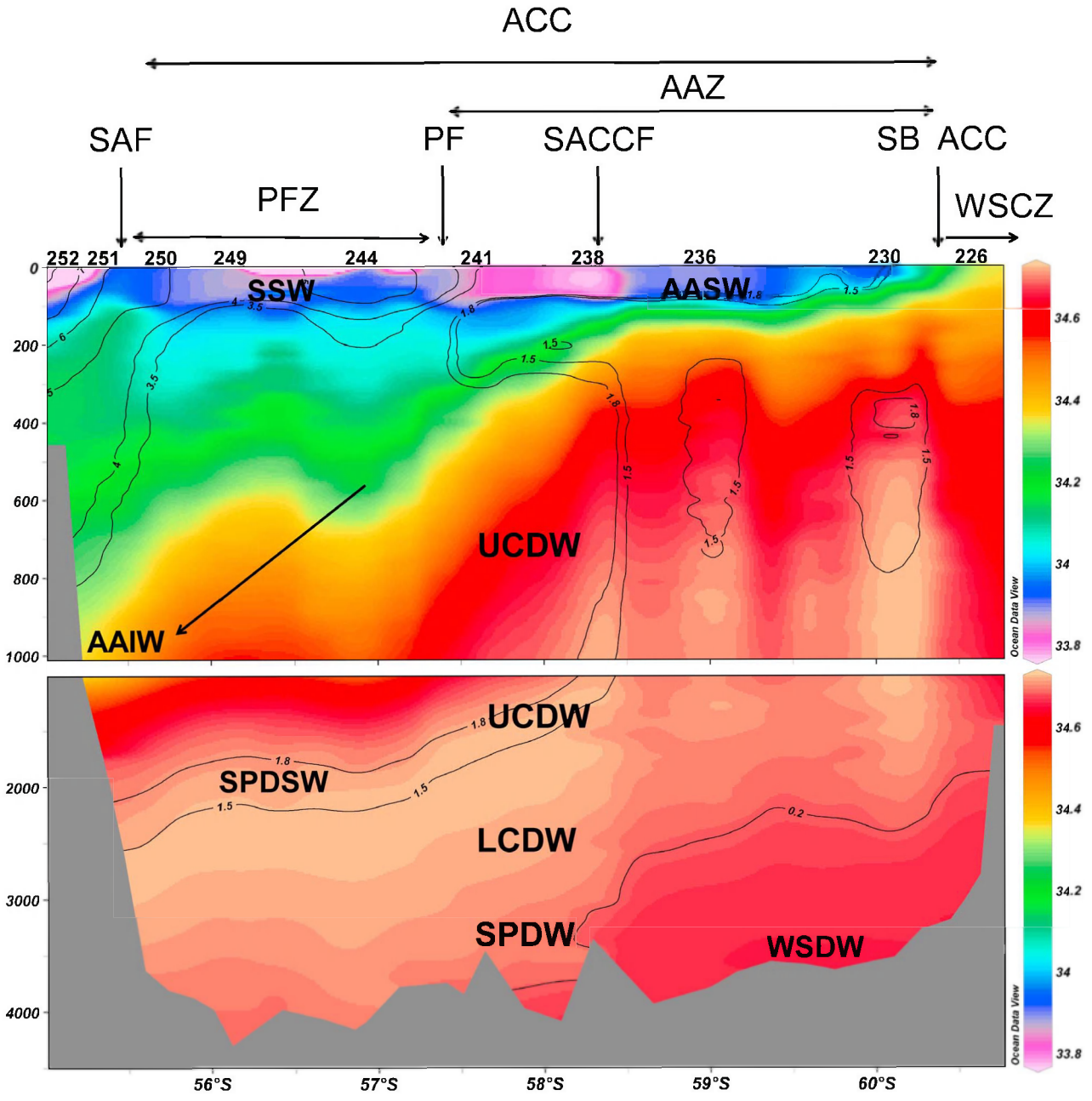

Figure 2. Water masses and fronts along the entire transect (see Figure 1). Salinity is represented in color scale and isolines represent the potential temperature (°C). (top) The upper 1000 m and (bottom) the remainder of the water column are shown. Abbreviations in alphabetical order: AAIW: Antarctic Intermediate Water (arrow indicates pathway of AAIW); AASW: Antarctic Surface Water ($\theta < 5$°C); AAZ: Antarctic Zone; ACC: Antarctic Circumpolar Current; LCDW: Lower Circumpolar Deep Water (0.2°C < θ < 1.8°C); PF: Polar Front; PFZ: Polar Frontal Zone; SACCF: Southern Antarctic Circumpolar Current Front; SAF: Sub-Antarctic Front; SB ACC: Southern Boundary of the Antarctic Circumpolar Current; SPDSW: Southeast Pacific Deep Slope Water; SPDW: South Pacific Deep Water; SSW: Sub-Antarctic Surface Water; UCDW: Upper Circumpolar Deep Water (1.5°C < θ < 3.5°C); WSCZ: Weddell Scotia Confluence Zone; WSDW: Weddell Sea Deep Water.

is the Circumpolar Deep Water (CDW). The CDW is commonly distinguished between Upper Circumpolar Deep Water (UCDW) and Lower Circumpolar Deep Water (LCDW). The UCDW is warmer and fresher than the LCDW which has a salinity maximum. Deeper than the LCDW, the South Pacific Deep Water with a maximum of silicate is observed. In the deepest parts of the southern Drake Passage, the lowest temperatures were associated with Weddell Sea Deep Water (WSDW) together with a decrease in the Si concentration [*Sudre et al.*, 2011]. In the northern

Drake Passage the Southeast Pacific Deep Slope Water (SPDSW) with a pronounced δ^3He maximum can be found toward to the continental slope of South America. These elevated δ^3He values are due to primordial helium originating from tectonically active mid-ocean ridges and hydrothermal activity in the Pacific [*Well et al.*, 2003].

4. Results and Discussion

4.1. Upper Water Column Distribution

[19] Surface [Al] was generally slightly elevated in the surface (upper 25 m) and underlain by a subsurface minimum. Contrarily, toward the Antarctic Peninsula and over the South American shelf, surface [Al] as well as surface [Mn] was elevated to considerably higher values (Figures 3 and 4). Near Elephant Island (station 226), [Al] was above 1 nM and near the South American continent (station 252), [Al] was extremely elevated to over 14 nM in the upper 20 m. When excluding those two stations, the average [Al] in the upper 25 m (Figure 5) of the remaining 8 stations was 0.39 nM (SD 0.21 nM; n = 8). Just north of the SACCF (station 238), the surface concentration was elevated to 1.28 nM (0.85 nM in upper 25 m) which is similar to the surface concentration near Elephant Island (Figure 5). However, at station 238 the [Al] decreased steeply with depth to a subsurface minimum of 0.23 nM at 100 m, while concentrations near Elephant Island remained around 1 nM with increasing depth. The Al surface enrichment at station 238 indicates an atmospheric source, corroborated by a surface enrichment that was observed for dissolved Fe (M. B. Klunder, PhD thesis in preparation, 2012). Contrarily, [Mn] was not elevated and one would expect a larger area to be affected by atmospheric input then just this one station, thus the origin of these elevated values remains unsure. Nevertheless, when also excluding this station with its relatively high [Al] surface concentration, the average decreases to 0.31 nM (SD 0.11 nM; n = 7) with a considerably lower standard deviation.

[20] A subsurface [Al] minimum was observed (Figures 6 and 7) around 100 m depth (95 ± 33 m), except at the two most southerly (stations 226 and 230) and the most northerly trace metal stations (station 252). When excluding these three coastal stations the average [Al] at the subsurface minimum was 0.18 nM (SD 0.05 nM). The relatively elevated surface [Al] compared to the subsurface minimum, indicates either a surface source, or increased scavenging by particles at the depth of the subsurface minimum. The latter appears not to be the case as two indicators of particle abundance, the fluorescence and coefficient of attenuation maximum, both are located at shallower depths. The only known surface source of Al to the open ocean is atmospheric dust input [e.g., *Measures and Vink*, 2000; *Measures et al.*, 2005]. However, even though [Al] is relatively elevated with respect to the subsurface minimum, it is lower than most reported [Al] in other ocean regions with known low dust input. In the Pacific Ocean, for example, elevated surface concentrations (followed by mid depth minima) are usually observed [e.g., *Orians and Bruland*, 1986; *Bruland et al.*, 1994; *Measures et al.*, 2005] and range between 0.3 nM and 8 nM. The average surface [Al] in the upper 25 m of the ice covered Arctic Ocean is considerably higher as well at 0.98 nM (n = 56 SD = 0.3 nM) [*Middag et al.*, 2009]. However, in the subarctic gyre of the North Pacific Ocean, *Measures et al.* [2005] reported surface water [Al] <0.1 nM for samples collected by a towed torpedo, but in the vertical profiles (collected with a CTD trace metal sampling system) surface [Al] was higher at ~1 nM [*Measures et al.*, 2005].

[21] In the Southern Ocean along the prime meridian, low surface concentrations and a subsurface minimum were observed as well [*Middag et al.*, 2011a], but both [Al] in the upper 25 m and at the subsurface minimum are higher (0.5 ± 0.15 nM and 0.33 ± 0.13 nM respectively), compared to Drake Passage. This seems inconsistent with the notion that surface [Al] is related to dust input as the modeled dust input in Drake Passage is higher than in the more remote Southern Ocean around the prime meridian [*Li et al.*, 2008, Figure 9; *Han et al.*, 2008, Figure 9b] due to the southeasterly pathway of the dust flux from Patagonia. However, the concentration of dissolved Al depends on dust input and solubility, but also on Al removal by scavenging processes [*Orians and Bruland*, 1986]. The lower [Al] in Drake Passage compared to the Southern Ocean prime meridian suggest a shorter residence time for Al in Drake Passage, consistent with model simulation results of *Han et al.* [2008, Figure 7].

[22] *Moran and Moore* [1992] suggested a first order dependence between oceanic scavenging rate constants for Al and ^{234}Th and suspended particle concentrations. The ^{234}Th distribution and depletion (with respect to ^{238}U) was, however, similar between Drake Passage and the prime meridian [*Rutgers van der Loeff et al.*, 2011]. Thus lower [Al] in Drake Passage cannot be attributed to more intense scavenging based on the ^{234}Th distribution and depletion. However, to draw conclusions for the scavenging of Al from the depletion and scavenging of ^{234}Th, the elements should have similar surface residence times in Drake Passage and along the prime meridian. Otherwise the distribution of Al could be affected by scavenging on a longer timescale than the distribution of ^{234}Th. The residence time for Al (~10 days to 4 years) overlaps with the residence time for ^{234}Th (days to weeks), but the spread for Al is much larger. Moreover, Al is not only scavenged, but also taken up by diatoms in the siliceous frustules as well [*Gehlen et al.*, 2002]. Therefore the ^{234}Th might not be as suitable as a proxy for Al scavenging by particles due to the different behavior of the two elements and more intense scavenging for Al in Drake Passage cannot be excluded.

[23] Alternatively, there may have been little dust input in the period prior to sampling or the modeled dust input to Drake Passage is over estimated, i.e., the prevailing winds are from the South Pacific Ocean and thus there is little dust input in Drake Passage. Using the MADCOW model [*Measures and Vink*, 2000] with an average mixed layer of 60 m, a 0.5 year surface ocean residence time for Al in Drake Passage [from *Han et al.*, 2008] and the average of the current measured [Al] in the upper 60 m (0.32 nM), yields an estimated dust input in the range of 0.25–0.85 g m^{-2} y^{-1} (using 1.5 and 5% solubility, respectively). This is about an order of magnitude lower than the estimated dust input by the DEAD model [*Han et al.*, 2008]. However, due to the underlying assumptions for the content and solubility of Al in dust and the residence time of dissolved Al these calculations are coarse estimates.

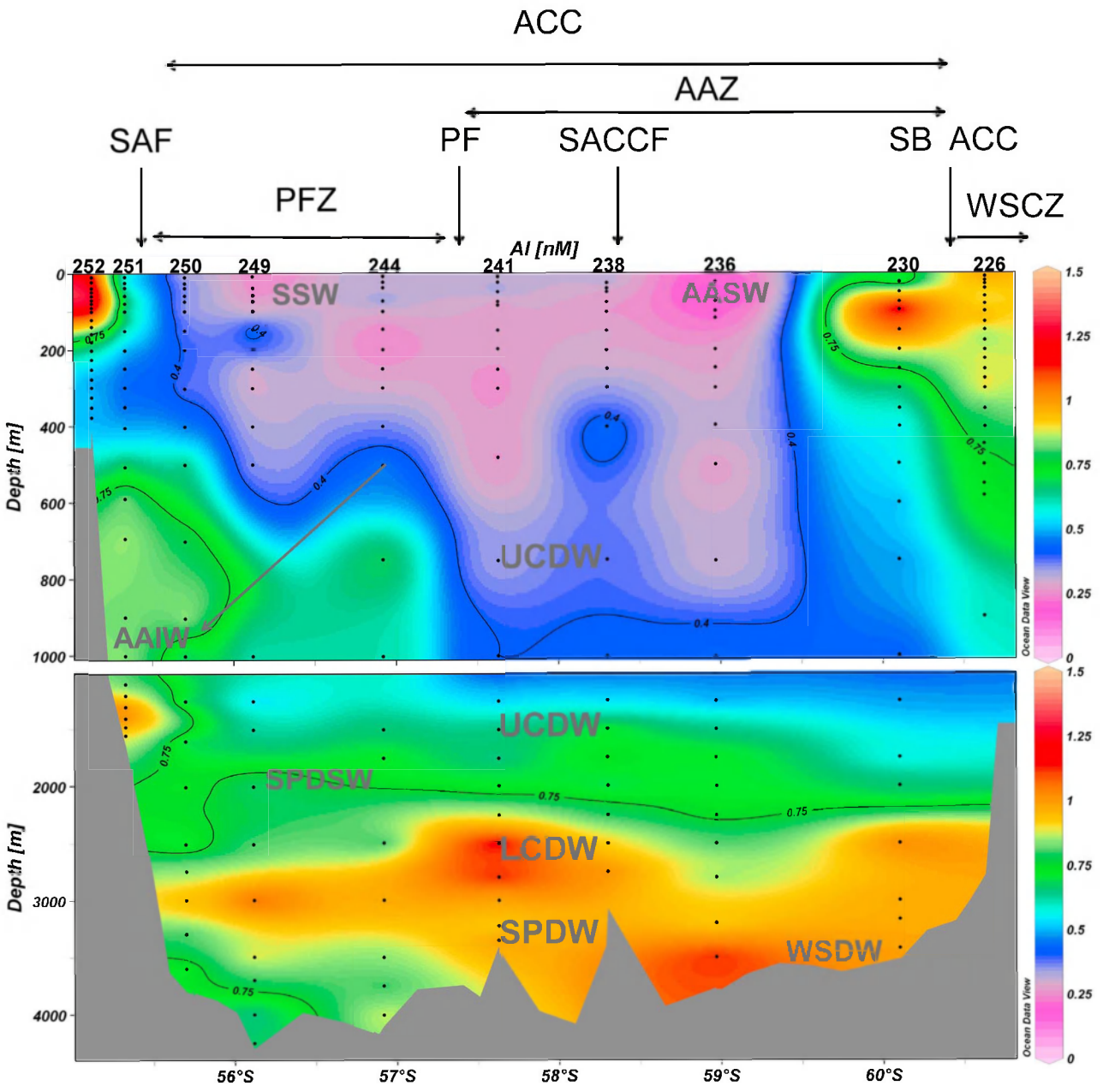

Figure 3. Concentrations of dissolved Al (nM) over the entire water column at all 10 TM stations crossing Drake Passage. (top) The upper 1000 m and (bottom) the remainder of the water column are shown. Stations numbers are indicated on top and isolines represent concentrations of Al. Of the 232 samples analyzed for Al, 18 samples (7.8%) were suspected outliers and therefore not further used in the figures. Abbreviations in alphabetical order: AAIW: Antarctic Intermediate Water (arrow indicates pathway of AAIW); AASW: Antarctic Surface Water; AAZ: Antarctic Zone; ACC: Antarctic Circumpolar Current; LCDW: Lower Circumpolar Deep Water; PF: Polar Front; PFZ: Polar Frontal Zone; SACCF: Southern Antarctic Circumpolar Current Front; SAF: Sub-Antarctic Front; SB ACC: Southern Boundary of the Antarctic Circumpolar Current; SPDSW: Southeast Pacific Deep Slope Water; SPDW: South Pacific Deep Water; SSW: Sub-Antarctic Surface Water; UCDW: Upper Circumpolar Deep Water; WSCZ: Weddell Scotia Confluence Zone; WSDW: Weddell Sea Deep Water.

[24] There are virtually no dissolved Al sources in the South Pacific Ocean and with the prevailing eastward flow of the ACC this means that the initial concentrations of Al (i.e., the concentrations of Al without the local dust input) are low in Drake Passage. In contrast, the easterly region along the prime meridian, downstream of the ACC and Weddell Gyre, could have received the accumulated dust deposition (i.e., the dust deposited upstream) from Patagonia as well as Al input from the continents and the continental margins of the Antarctic Peninsula and South America (see sections 4.1.1

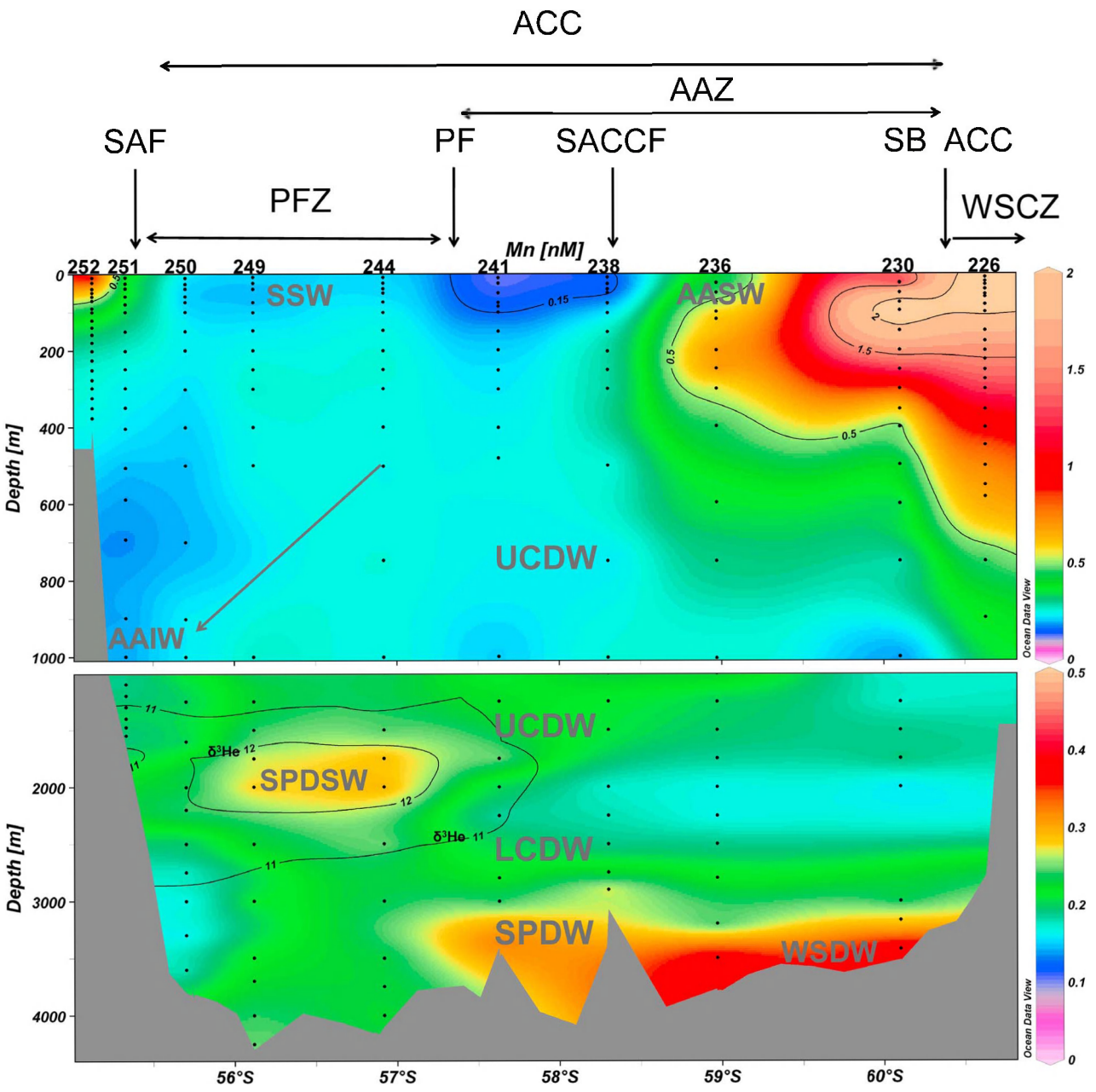

Figure 4. Concentrations of dissolved Mn (nM) over the entire water column at all 10 TM stations crossing Drake Passage. (top) The upper 1000 m is shown with isobars indicating the concentration of Mn. (bottom) The remainder of the water column is shown in a different color scheme with isolines indicating the values of δ^3He. Stations numbers are indicated on top. Of the 232 samples analyzed for Mn, 12 samples (5.2%) were suspected outliers and therefore not further used in the figures. Abbreviations in alphabetical order: AAIW: Antarctic Intermediate Water (arrow indicates pathway of AAIW); AASW: Antarctic Surface Water; AAZ: Antarctic Zone; ACC: Antarctic Circumpolar Current; LCDW: Lower Circumpolar Deep Water; PF: Polar Front; PFZ: Polar Frontal Zone; SACCF: Southern Antarctic Circumpolar Current Front; SAF: Sub-Antarctic Front; SB ACC: Southern Boundary of the Antarctic Circumpolar Current; SPDSW: Southeast Pacific Deep Slope Water; SPDW: South Pacific Deep Water; SSW: Sub-Antarctic Surface Water; UCDW: Upper Circumpolar Deep Water; WSCZ: Weddell Scotia Confluence Zone; WSDW: Weddell Sea Deep Water.

and 4.1.2). This influence was also shown by *Hegner et al.* [2007] from neodymium isotope data, indicating Patagonia and the Antarctic Peninsula provide material that is transported east with the ACC and Weddell Gyre. It has been suggested that Al from derived re-suspended sediments near continental margins can be transported over large distances across the Pacific with the equatorial undercurrent [*Kaupp et al.*, 2011]. Thus it is not unlikely that Al input from the

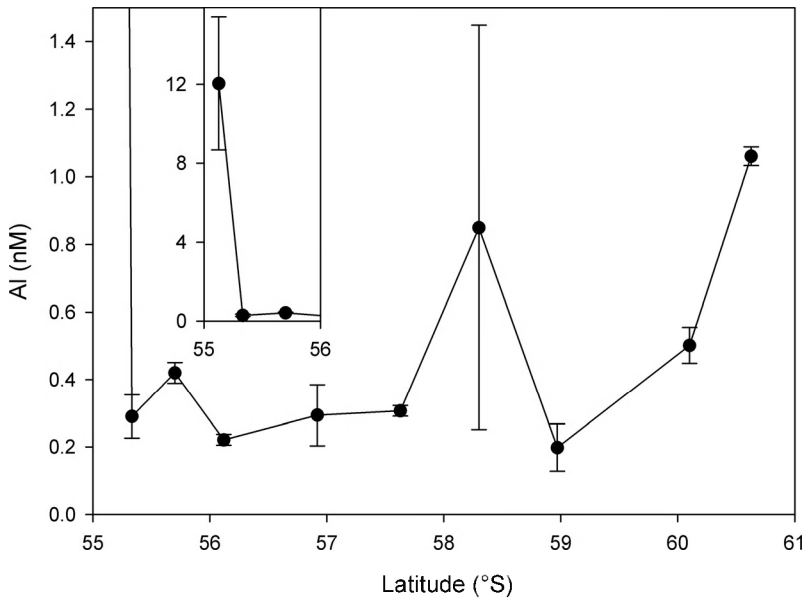

Figure 5. Concentrations of dissolved Al (nM) averaged over the upper 25 m along the transect; station numbers are indicated on the plot. Error bars represent the standard deviation of the averaged concentrations of 10 and 25 m depth, each measured in triplicate. Inset at upper left shows stations 252, 251 and 250 at expanded scale.

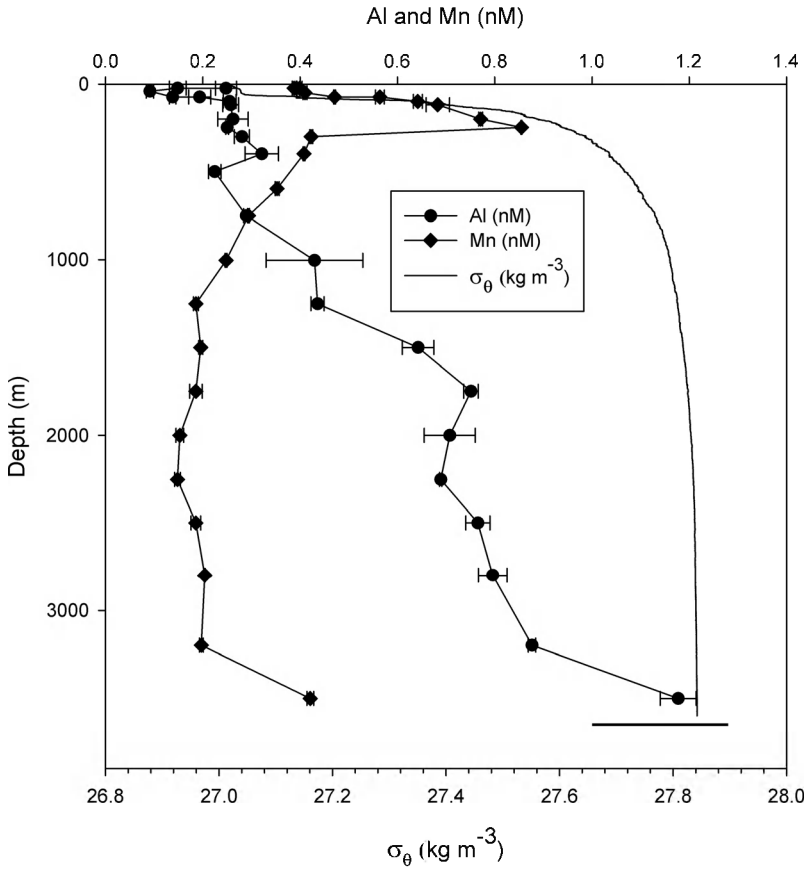

Figure 6. Concentrations of Al (nM) (circles) and Mn (nM) (diamonds) and σ_θ (kg·m^{-3}) (solid line) as vertical profile versus depth in the southern Drake Passage (station 236, south of the SACCF). Error bars represent standard deviation of triplicate measurements. Bottom depth is indicated by a solid line.

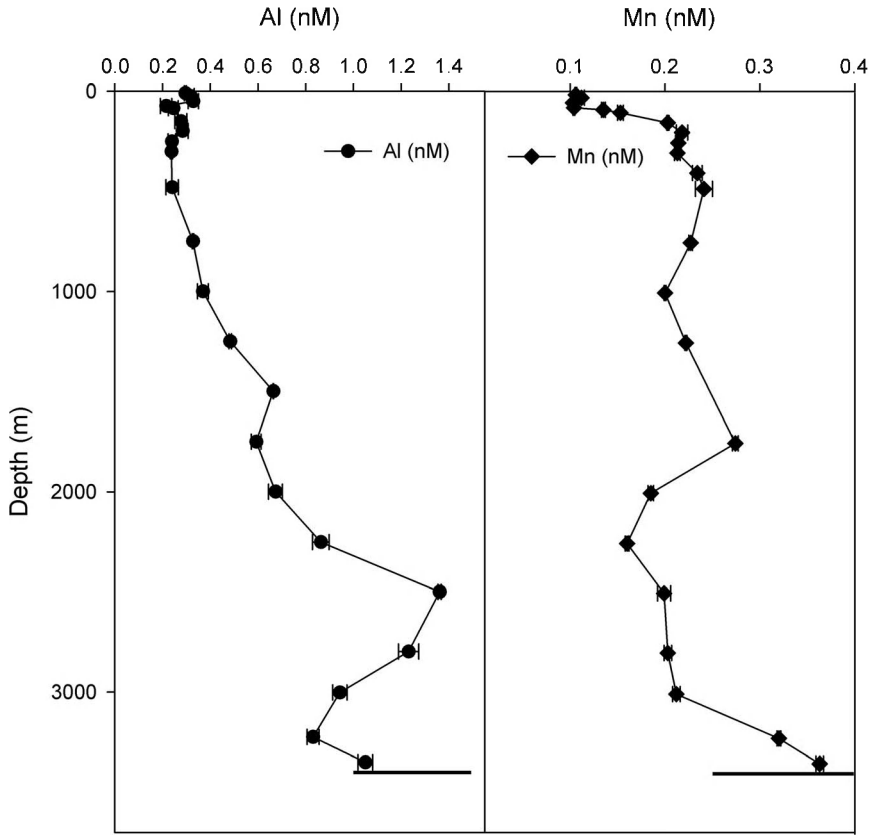

Figure 7. Concentrations of Al (nM) (circles) and Mn (nM) (diamonds) as vertical profile versus depth in the northern Drake Passage (station 241, just south of PF). Error bars represent standard deviation of triplicate measurements. Bottom depth is indicated by a solid line.

continental margins of Drake Passage and the accumulated dust deposition is responsible for the higher [Al] observed along the prime meridian.

[25] Within the ACC, surface [Mn] was much lower than near the Peninsula or South American continent (see below) and a subsurface maximum was observed. Surface concentrations were lowest (~0.1 nM) between the SACCF and PF with subsurface maxima of 0.25 nM at 200 m depth for station 238 and 0.22 nM at 200 m depth at station 241 (Figure 7). This is comparable to results reported by *Martin et al.* [1990], who reported 0.08 nM in the surface and 0.22 nM at 110 m depth. Lowest surface [Mn] coincided with elevated fluorescence and the $^{234}Th/^{238}U$ ratio showed highest export [*Rutgers van der Loeff et al.*, 2011], indicating biological export of Mn. The [Mn] in source waters (i.e., water upstream in the Pacific sector of the ACC) is most likely a factor as well in the very low observed concentrations between the PF and SBACCF. However, the higher [Mn] of the subsurface maximum (and deeper), compared to the surface layer, cannot be explained by advection of low [Mn] water into this region. The current observations can only be explained if there is a sink for Mn in the surface layer. This is most likely due to active biological uptake as extensively discussed by *Middag et al.* [2011c], where a similar surface distribution of Mn is described over a much larger area along the Prime Meridian. Subsurface maxima observed in that region, were suggested to be related to remineralization at this depth [*Middag et al.*, 2011c]. Surface water [Mn] of ~0.2 nM in the PFZ was slightly higher than between the SACCF and the PF, but subsurface maxima of 0.26 nM at 100 m depth and 0.28 nM at 300 m depth (stations 244 and 249, respectively) were observed. This indicates Mn uptake in the surface layer and remineralization just below plays a role in the PFZ as well, but closer toward the SAF this phenomenon becomes less clear.

4.1.1. South American Side

[26] At the South American continental shelf break (station 252) surface [Mn] and [Al] were highest (2.3 nM and >14 nM respectively). However, both concentrations decreased steeply with increasing depth in the shallow (~410 m) water column to 0.25 nM and 0.45 nM, respectively, for [Mn] and [Al] (Figure 8). This indicates a surface source, but no significant flux of Mn and Al from the sediments. In the fresh (salinity < 34) upper 150 m (σ_θ ranging from 25.37 to 26.59 kg·m^{-3}), [Mn] and [Al] were inversely correlated with salinity (R^2 = 0.99; n = 10; P < 0.001; see Figure 8 caption) and positively correlated with each other (R^2 = 0.99; n = 10 and P < 0.001; see Figure 8 caption), indicating conservative mixing and a common source in the upper water column. The surface source could be atmospheric input or land run-off, but given the correlation with salinity, land run-off is the most likely source. Although this land run-off input resulted in very high [Al] of almost 15 nM in the upper waters over the shelf, [Al] decreased with distance (<0.4 nM over the continental slope (station 251, Figure 5)) and depth. This extreme gradient in [Al] of over

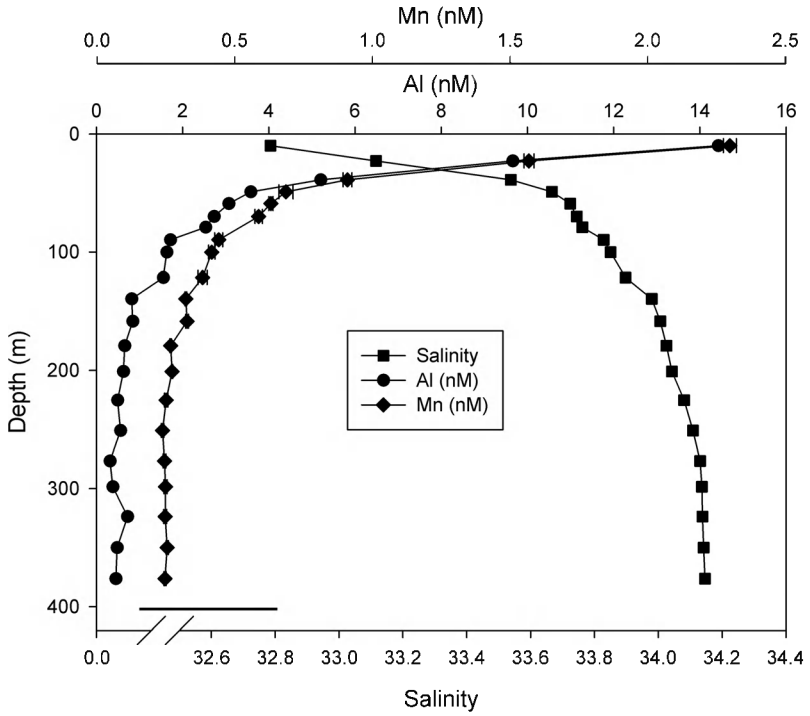

Figure 8. Concentrations of Al (nM) (circles), Mn (nM) (diamonds) and salinity (squares) as vertical profiles versus depth over the South American continental shelf (station 252). Error bars represent standard deviation of triplicate measurements. Standard deviations of the triplicate analysis of Al were on average 3.6% and therefore not visible on this scale. Bottom depth is indicated by a solid line. The concentrations of Mn and Al are inversely correlated with salinity in the upper 150 m of the water column and described by [Al] (nM) = −11.46*salinity + 389.7 with R^2 = 0.99, n = 11 and $P < 0.001$; [Mn] (nM) = −1.66*salinity + 56.7 with R^2 = 0.99, n = 10 and $P < 0.001$. The relationship between Al and Mn in the upper 150 m of the water column is described by [Al] (nM) = 6.87*Mn (nM) − 1.2 with R^2 = 0.99, n = 10 and $P < 0.001$.

1 order of magnitude is consistent with the reported behavior of Al brought into the oceans with land run-off. The bulk of the dissolved Al delivered by rivers precipitates in the estuary due to flocculation, authigenic aluminosilicate formation and consumption of Al at the sediment water interface [*Mackin and Aller*, 1984a, 1984b, 1986]. This would explain the low [Al] observed near the sediments of the South American shelf (Figure 8) compared to the concentrations in the deep Drake Passage (Figure 3). However, intensive scavenging unrelated to estuarine processes (e.g., by diatoms) cannot be excluded either as the large spatial [Al] gradient (>14 nM to <0.4 nM) was observed over a comparatively small salinity gradient (32.8 to 33.9) between station 252 (shelf) and 251 (slope). Like surface [Al], surface [Mn] decreases toward Drake Passage to concentrations (0.15 nM in the upper 100 m of station 251) that are lower than expected based on conservative mixing. This indicates a sink for [Mn], which is most likely biological uptake as suggested above. Moreover, influence of land run-off apparently did not extend beyond the surface layer of the shelf sea.

[27] Both higher [Al] and [Mn] were observed near the sediments of the continental slope around 1300–1400 m depth (station 251). Just south of the SAF (station 250), an Al maximum of 0.9 nM was observed around 900 m depth (σ_θ 27.49 kg·m^{-3}), coinciding with the core of the AAIW (see section 3). Contrarily, [Mn] appears lower at this depth (Figure 4), but this is related to the higher concentrations at the subsurface maxima and the underlying SPDSW (see section 4.2.4). In the vertical profile there is actually a small [Mn] maximum (0.23 nM) at 900 m depth at this station. There is no apparent reason why the AAIW should have higher [Al] and [Mn], nor was there an [Al] or [Mn] maximum at the depth of the AAIW at other stations. Dissolved Mn can be released from (reducing) shelf sediments [*Heggie et al.*, 1987; *Sundby and Silverberg*, 1985; *Johnson et al.*, 1992; *Pakhomova et al.*, 2007], but undisturbed sediments (i.e., no re-suspension) have been reported to act as a sink for dissolved Al [*Mackin and Aller*, 1984a, 1984b]. Thus the combination of elevated deep [Al] and [Mn] suggests re-suspension of sediment (with subsequent dissolution of Al and Mn) and Al and Mn rich pore waters. This process of re-suspension appears to elevate the trace metal concentrations near the South American continental slope. Contrarily, sediments of the shallow shelf sea do not appear to be a source of Al and Mn (Figure 8), and possibly even a sink for Al.

4.1.2. Peninsula Side

[28] Near Elephant Island (station 226), [Mn] was elevated in the surface layer (σ_θ 27.52–27.57 kg·m^{-3}) to over 2 nM and the coefficient of attenuation was relatively high (Figure 9). Farther into Drake Passage (station 230), surface

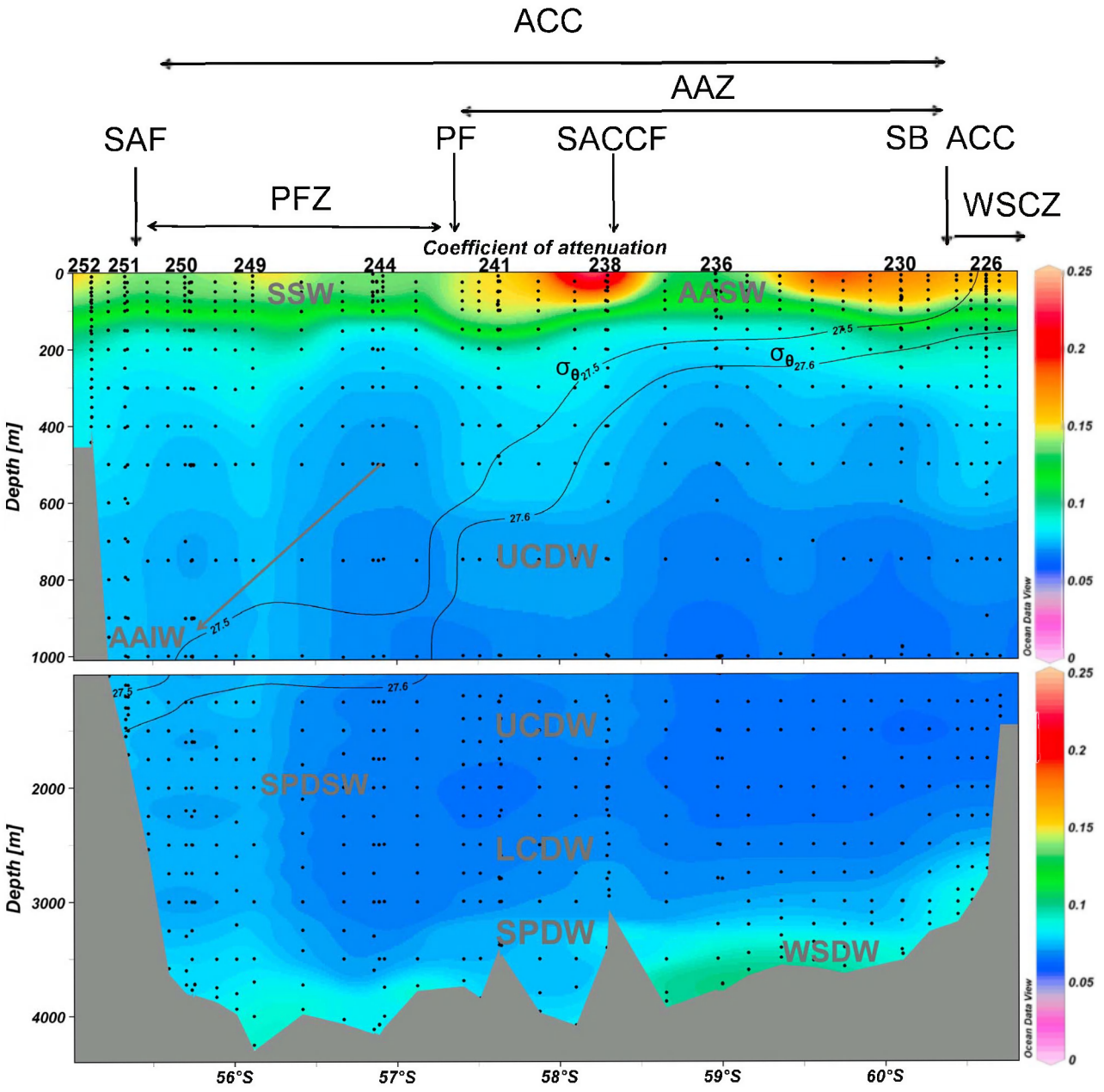

Figure 9. Coefficient of attenuation over the entire water column at all 10 stations crossing Drake Passage with isolines indicating σ_θ (kg·m^{-3}). (top) The upper 1000 m and (bottom) the remainder of the water column are shown. Stations numbers are indicated on top. Abbreviations in alphabetical order: AAIW: Antarctic Intermediate Water (arrow indicates pathway of AAIW); AASW: Antarctic Surface Water; AAZ: Antarctic Zone; ACC: Antarctic Circumpolar Current; LCDW: Lower Circumpolar Deep Water; PF: Polar Front; PFZ: Polar Frontal Zone; SACCF: Southern Antarctic Circumpolar Current Front; SAF: Sub-Antarctic Front; SB ACC: Southern Boundary of the Antarctic Circumpolar Current; SPDSW: Southeast Pacific Deep Slope Water; SPDW: South Pacific Deep Water; SSW: Sub-Antarctic Surface Water; UCDW: Upper Circumpolar Deep Water; WSCZ: Weddell Scotia Confluence Zone; WSDW: Weddell Sea Deep Water.

[Mn] was still relatively high around 0.7 nM, followed by a subsurface maximum of 2.6 nM at 75–95 m depth at a σ_θ of 27.50 kg·m^{-3} (Figure 10). Concentrations of dissolved Al and iron (Klunder, PhD thesis in preparation, 2012) were elevated in the upper waters near the Antarctic Peninsula as well, but [Al] to much lower concentrations (~1 nM) than on the South American side (Figure 3). Moreover, surface salinity was much higher (>34, not shown), thus land run-off was apparently not as significant a process near the Antarctic Peninsula. The vertical profiles of [Mn], [Al] and σ_θ together (station 230, Figure 10), indicate that Mn and Al from the Peninsula shelf and slope protrude into the ACC along the

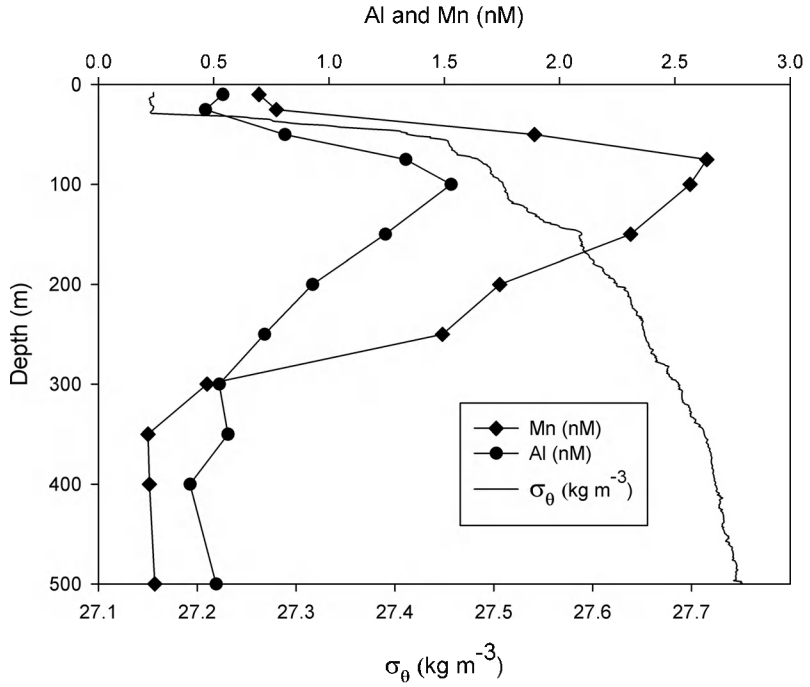

Figure 10. Concentrations of Al (nM) (circles) and Mn (nM) (diamonds), σ_θ (27.49 kg·m^{-3}) (solid line) as vertical profiles versus depth just north of the SB ACC (station 230). Standard deviations of triplicate analysis were on average 1% for Mn and 3.5% for Al and therefore not visible on this scale. The distinct maxima of Al and Mn at ~100m depth are ascribed to transport from the Antarctic Peninsula along the ~27.5 kg·m^{-3} isopycnal, see main text.

~27.5 kg·m^{-3} isopycnal (Figure 9). The advection of high [Al] and [Mn] into Drake Passage is also visualized in the color plots (Figures 3 and 4). The source of the elevated [Al] and [Mn] is most likely sediment re-suspension, given there is no evidence for land run-off.

[29] Farther north at station 236, a strong increase with depth to a subsurface maximum of 0.77 nM [Mn] at 200m (σ_θ 27.56 kg·m^{-3}) and 0.86 nM [Mn] at 250m (σ_θ 27.61 kg·m^{-3}) was still observed, however without a corresponding maximum in [Al] (Figure 6). This indicates Mn input from sediment re-suspension penetrates farther from the peninsula into the ACC (Stations 230 and 236) along the ~27.5–27.6 isopycnal (Figure 9) than Al input. Most likely the Al scavenging by particles is faster than the oxidative scavenging of Mn. The influence of sediment re-suspension from either the Peninsula or the South American continent does not affect the distribution of Al and Mn anymore in the middle Drake Passage. However, with the flow direction of the ACC being more or less perpendicular to this transect, the influence on the Al and Mn distribution downstream might be greater than can be concluded from this study.

4.2. Deep and Intermediate Distribution

[30] In the deep and intermediate water layers of Drake Passage, [Mn] is not as low and uniform as often observed in other ocean basins (see section 4.3). Lowest [Mn] at mid-depth was around 0.15 nM, which is comparable to concentrations observed in the ACC along the prime meridian, but higher than in the Weddell Gyre [*Middag et al.*, 2011c]. Elevated [Mn] was observed in the deepest water layers of Drake Passage (Figure 4), especially in the southern Drake Passage where WSDW influence has been suggested (see section 3). Furthermore, mid-depth maxima in the concentration of Mn were observed in the northern Drake Passage (Figure 4) where influence of SPDSW has been shown [*Well et al.*, 2003]. In the intermediate water column, [Al] generally increased gradually with depth below the subsurface minimum (Figures 6 and 7). Similar to [Mn], [Al] increased relatively steeply (>1 nM) in the southern Drake Passage with WSDW influence (Figure 3).

4.2.1. WSDW Influence

[31] The influence of WSDW is visible in various tracers like nutrients, oxygen and low potential temperature, θ (Figure 2). When plotting [Mn] versus θ deeper than 3000 south of the SACCF, indeed a significant correlation (P = 0.01) appears (not shown). This indicates the higher [Mn] (~0.4 nM) in the deep southern Drake Passage is related to the influence of the WSDW. However, [Mn] in the WSDW in the Weddell Gyre was actually much lower, around 0.1 nM [*Middag et al.*, 2011c]. Similarly, just the influence of WSDW cannot account for the elevated [Al] in the deep southern Drake Passage, as [Al] observed in WSDW in the Weddell Gyre was lower (0.3–1 nM) [*Middag et al.*, 2011a]. In the cold and dense Weddell Sea Bottom Water (WSBW) [Mn] was only slightly higher (0.15 nM), but [Al] in the same range (1–1.5 nM) as in the deep southern Drake Passage was observed [*Middag*, 2010; *Middag et al.*, 2011a, 2011c]. However, there is no evidence suggesting a significant influence of WSBW in the deep Drake Passage and any WSBW influence would only be a fraction of the water present in the deep southern Drake Passage, thus unable to

cause the elevated [Al] observed. The elevated [Mn] in the deep southern Drake Passage appear not to be of hydrothermal origin as then the δ^3He should be elevated as well [*Klinkhammer et al.*, 2001], which was not observed.

[32] However, the coefficient of attenuation increased as well in the WSDW influenced deep southern Drake Passage (Figure 9). According to *Sudre et al.* [2011], the WSDW is propagated along the continental slope from the Weddell Sea into the southern Drake Passage. During this transport along the slope, apparently particles are getting suspended, thereby increasing the coefficient of attenuation. Subsequent partial dissolution of these particles and the input of Al and Mn rich pore water are then the most likely source of the elevated [Mn] and [Al] associated with this WSDW influence.

4.2.2. North Atlantic Deep Water Influence

[33] In the northern Drake Passage, like in the southern Drake Passage, [Al] increased gradually with depth below the subsurface minimum. However, highest concentrations (up to 1.3 nM) were usually not observed at the greatest sampled depth, but between 2500 and 3000 m depth, several hundreds of meters above the seafloor (Figure 7). The deep Al maxima rise from around 3000 m depth at the most northerly stations to around 1750 m southwards of the SACCF (Figure 6). The maxima also became less profound in the southward direction. The depths of these Al maxima correspond with the depth range of LCDW [*Sudre et al.*, 2011] that has a salinity maximum due to the influence of North Atlantic Deep Water (NADW). In the ACC along the prime meridian, Al maxima corresponded with the NADW salinity maximum, suggesting the Al-rich NADW is the source of the Al maxima [*Middag et al.*, 2011a]. In Drake Passage, the Al maxima were much lower than the maxima of up to 6 nM observed along the prime meridian. The lower Al maxima are not surprising as the influence of NADW is less in Drake Passage, showing in the lower LCDW salinity in Drake Passage compared to the prime meridian. The Al and salinity maxima are somewhat vertically resolved in Drake Passage; Al maxima were observed just under the salinity maxima. This is most likely related to the concentrations of Al in the overlying UCDW and underlying SPDW. Mixing of LCDW with overlying, relatively Al-poor, UCDW and underlying, relatively Al-rich, SPDW results in an Al maximum located toward the deeper part of the LCDW, closer to the SPDW than to the UCDW. This fits the observed distribution of Al in the deep Drake Passage, indicating the Al maxima in the deep Drake Passage, although vertically resolved from the salinity maximum, are related to NADW influence. The NADW influence does not appear to influence the Mn distribution notably, as NADW generally has low uniform [Mn] in the same range (~0.15 nM) [*Statham et al.*, 1998] as observed in the intermediate water column of Drake Passage.

4.2.3. Bottom Sediments Influence

[34] In the deep northern Drake Passage an [Al] increase toward the sediments was observed (Figure 7). Similarly, [Mn] was relatively elevated at the greatest sampled depths farther north than the extent of the influence of the WSDW (Figure 4). However, [Mn] in the range of 0.2–0.3 nM, was not as high as in the region with WSDW influence. In the deepest water layers of Drake Passage no low oxygen saturations were encountered (all > 60%). An in situ Mn flux from undisturbed (not re-suspended) underlying sediments is very unlikely. The oxygen penetration of deep ocean sediments is usually well over 1 m and pore water [Mn] is therefore relatively low in the upper sediment [e.g., *Rutgers van der Loeff et al.*, 1990] and Mn does not escape the sediment water interface [*Pakhomova et al.*, 2007]. Even though [Mn] in pore waters is relatively low in oxygenated deep sea sediments, concentrations are higher than in the overlying water column. Re-suspension of sediments could therefore elevate the water column [Mn] via direct input of pore water and partial dissolution of sediment particles as seen near the continental margins.

[35] It has been suggested biogenic silica in sediments acts as a filter for Al, preventing large Al fluxes from the ocean sediments, especially in the Southern Ocean [*Van Beueskom et al.*, 1997]. However, pore water [Al] in the deep Southern Ocean is much higher (up to 2 orders of magnitude [*Van Beueskom et al.*, 1997]) than in the overlying water column. Thus re-suspension of bottom sediments and pore water could definitely be a source of dissolved Al to the overlying water column. Besides high [Mn] and [Al], the coefficient of attenuation increased in the deep northern Drake Passage as well (Figure 9), but not as much as in the southern Drake Passage. These higher [Mn], [Al] and coefficient of attenuation indicate particles (and associated pore water) from the seafloor get re-suspended by the currents of the ACC through Drake Passage. All three parameters get elevated after sediment re-suspension, but even after particles have settled, trace metal concentrations remain elevated and diffuse away, giving rise to the somewhat different distribution between the attenuation coefficient and [Al] and [Mn]. The attenuation merely serves as an indicator sediment re-suspension is happening. Furthermore, [Al] and [Mn] are affected differently by re-suspension of sediment (e.g., input concentration and respective scavenging intensities) and thus have differences in their distributions as well. Bottom velocities of the ACC in Drake Passage are poorly known, but thought to be significant [*Lenn et al.*, 2008] and based on the data presented here, apparently capable of re-suspending sedimentary particles.

4.2.4. SPDSW Influence

[36] North of the SACCF, elevated [Mn] was observed in the 1500–2200 m depth range (Figure 2). The actual maxima (0.25 to 0.32 nM) were found between 1750 m (station 241) and 2200 m depth (station 250). This depth range coincides with the influence of SPDSW and its δ^3He maximum from Pacific origin [*Well et al.*, 2003; *Sudre et al.*, 2011]. Plotting [Mn] versus δ^3He for the 1500 to 2500 m depth range between the SAF and SACCF (Figure 11) yields a robust correlation ($[Mn] = 0.03*[\delta^3He] - 0.11$ with $R^2 = 0.7$; $n = 19$ and $P < 0.0001$).

[37] Outside the depth range where significant percentages of SPDSW are usually found [*Sudre et al.*, 2011], [Mn] and δ^3He appear not to be related. The correlation observed within the SPDSW influenced part of the water column is therefore a convincing indicator of a common source of the elevated [Mn] and δ^3He. As δ^3He is, like Mn, released at spreading mid-ocean ridges and via hydrothermal vents [*Farley et al.*, 1995; *Klinkhammer and Hudson*, 1986], it appears the elevated [Mn] at mid-depth in the northern Drake Passage is from volcanically active ridges in the Pacific Ocean that the SPDSW has passed on its way to Drake Passage.

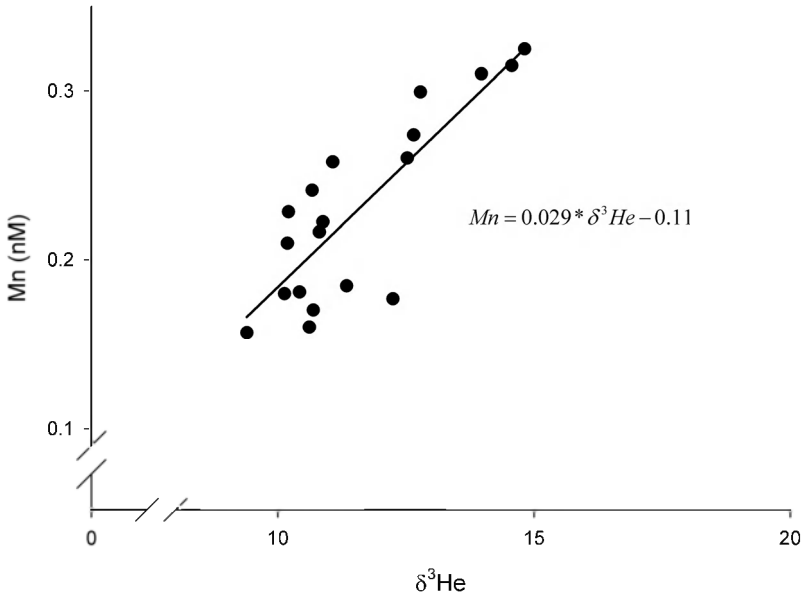

Figure 11. Concentrations of dissolved Mn (nM) versus δ^3He in the northern Drake Passage for the 1500 to 2500 m depth range. Dissolved Mn and δ^3He were sampled at different casts, thus depths are not identical. However, all points used for this relation ($R^2 = 0.70$; n = 19; $P < 0.001$) were within 100 m depth from each other. At one exception (around 56°S in the PFZ), dissolved Mn and δ^3He data (4 data points) from two different stations were used as they were not sampled at the same station. The [Mn] data is from station 249 and the δ^3He from station 248 (Table 1) which are merely 20 miles apart.

4.3. Comparison With Previously Reported Data and Other Ocean Basins

4.3.1. Aluminum

[38] Very little data has been reported thus far on concentrations of dissolved Al in Drake Passage. *Hewes et al.* [2008] reported averaged concentrations of dissolved Al of the upper water column for different water zones in the Weddell-Scotia Confluence. They used an epoxy-coated aluminum rosette frame with GO-FLO bottles and reported an [Al] of 2.0 nM (±0.4 nM) for the upper 60 m along the shelf and shelf-break of Elephant Island (their water zone 3). When averaging the upper 60 m from the station just north of the shelf-break from this study (station 226), [Al] is 0.95 nM (±0.11 nM) - a much lower value. In Drake Passage south of the PF, an average [Al] of 1.2 nM (±0.3 nM) was reported by *Hewes et al.* [2008] for the upper 150 m (their water zone 1A). This is also considerably higher than the average concentration of 0.29 nM (±0.07 nM) for the upper 150 m between the PF and SACCF from this study. There appears to be an offset of about 1 nM between [Al] reported by *Hewes et al.* [2008] and the data from this study. Such an offset might be related to temporal and spatial differences or temporal events like dust input, but this remains speculation. Otherwise, this apparent offset stresses the importance of rigorous use (and reporting of results) of standard reference samples such as the GEOTRACES or SAFe reference samples, as was done in this study (http://www.geotraces.org/science/intercalibration).

[39] *Van Bennekom et al.* [1991] report a vertical profile of unfiltered Al in the Scotia Sea somewhat further east (at 57°S, 49°W), collected by GO-FLO bottles on a coated stainless steel rosette frame. The general trend of the reported profile is similar to the observations in this study; an increase with depth from relatively low surface values to higher concentrations in the deep. However, the actual concentrations are much higher in the range of 1–3 nM compared to the range of 0.1–1.5 nM found in this study. Higher concentrations for unfiltered samples are expected, but this difference is thought to be in the order of 10% [*Measures*, 1999]. The reported precision (0.3 nM) reported by *Van Bennekom et al.* [1991], is in the range of the actual Al values in this study, thus precluding comparison between the two data sets.

[40] Surface [Al] in Drake Passage are some of the lowest [Al] observed anywhere. To the best of our knowledge the only other concentrations this low are those reported for the HNLC waters of the Pacific subarctic gyres [*Orians and Bruland*, 1988; *Measures et al.*, 2005; *Brown et al.*, 2010], parts of the California Current [*Orians and Bruland*, 1986] and the Atlantic sector of the Southern Ocean [*Middag et al.*, 2011a]. However, the shape of the vertical profiles of [Al] in the low [Al] Pacific Ocean regions usually showed a mid-depth minimum, unlike the profiles observed in Drake Passage. So even though the concentration range is similar, different processes appear to control the distribution of Al in Drake Passage compared to the low [Al] Pacific Ocean regions. The profile shapes observed in Drake Passage and in the ACC further east along the prime meridian [*Middag et al.*, 2011a] are more similar. However, surface concentrations in the ACC along the prime meridian were slightly higher than in Drake Passage (see section 4.1.) and the NADW influence was less profound in Drake Passage. This indicates similar processes control the distribution of Al in Drake Passage as in the Southern Ocean more to the east, but local differences like for example scavenging intensity,

variability in input sources and variability in concentrations of Al in source waters remain.

4.3.2. Manganese

[41] Like for [Al], very little data has been reported on [Mn] thus far on the Drake Passage. Findings of *Martin et al.* [1990] are in agreement with the current observations (see section 4.1). *Westerlund and Öhman* [1991] reported dissolved Mn on the eastern side of the Peninsula (Weddell Sea) with some stations close to the Antarctic Peninsula. Surface [Mn] reported there by *Westerlund and Öhman* [1991] is lower (around 0.4 nM) than the currently reported [Mn] on the Drake Passage side. Similarly, surface [Mn] observed on the eastern side [*Middag*, 2010] during the same cruise as the currently reported Drake Passage data, was much lower (~0.8 nM over the shelf and ~0.26 nM over the slope). This indicates the surface enrichment near Elephant Island is a local phenomenon. Very similar concentrations were observed in the deep at the onset of both continental slopes on the eastern (station 44 of *Westerlund and Öhman* [1991]) and Drake Passage side of the Peninsula (station 230), with an average absolute deviation for similar depths of only 0.04 nM.

[42] For Drake Passage south of the PF, *Hewes et al.* [2008] reported an average [Mn] of 0.17 ± 0.07 nM for the upper 150m (their water zone A). This concentration is nearly identical to the current average [Mn] of 0.13 nM (±0.05 nM) for the upper 150 m between the PF and SACCF. The reported average [Mn] of 2.47 nM (±0.23 nM) for the upper 60 m along the shelf and shelf-break of Elephant Island (their water zone 3) is also very similar to the average [Mn] of 2.23 nM (±0.02 nM) for the upper 60 m just north of the shelf-break from this study (station 226). This confirms that indeed [Mn] is generally much higher on the Drake Passage side compared to the data reported for the eastern side of the Peninsula.

[43] The [Mn] profile shape of the most southerly (station 226) and most northerly (station 252, Figure 8) stations in Drake Passage, is comparable with the general profile shape in the other major ocean basins. For example, in the Pacific Ocean [e.g., *Landing and Bruland*, 1980, 1987], Atlantic Ocean [e.g., *Bruland and Franks*, 1983; *Jickells and Burton*, 1988; *Landing et al.*, 1995; *Saager et al.*, 1997; *Shiller*, 1997], Indian Ocean [e.g., *Saager et al.*, 1989; *Morley et al.*, 1993] and Arctic Ocean [e.g., *Yeats*, 1988; *Middag et al.*, 2011b] the [Mn] profile generally shows elevated surface concentrations and low uniform deep values. At the remaining stations of Drake Passage however, the surface concentrations were not elevated, but either depleted or similar to the remainder of the water column. This indicates a lack of surface sources of Mn in the middle Drake Passage, likely in combination with biological uptake of Mn as observed in the ACC along the prime meridian [*Middag et al.*, 2011c]. The dissolved Mn surface concentrations in Drake Passage are, like the [Al], among the lowest [Mn] observed anywhere. To the best of our knowledge, only in the Southern Ocean comparable [Mn] has been reported [*Martin et al.*, 1990; *Westerlund and Öhman*, 1991; *Sedwick et al.*, 1997, 2000; *Middag et al.*, 2011c].

[44] Like the surface water distribution, the deep water distribution is different from the general ocean distribution (low and relatively uniform deep [Mn]). The Drake Passage is influenced by WSDW inflow, sediment re-suspension and hydrothermal influence (see section 4.2), creating the unique deep Mn distribution in this narrow channel with high energy levels.

5. Conclusions

[45] The distribution of Al in Drake Passage is influenced by fluxes from the continental margins, by advection, and perhaps variations in scavenging intensity in surface waters on a relatively small spatial scale. The distribution of Mn in the Drake Passage is influenced by fluxes from the continental margins, by advection and by biological uptake in the surface layer. Lowest [Mn] was observed between the SAF and SACCF and these lower concentrations were most likely due to biological uptake. Highest [Al] and [Mn] were observed in surface waters close to the South American continent and are related to land run-off. However, these elevated concentrations disappear with depth over the water column and with distance into Drake Passage. This shows land run-off is only of influence over the shelf and does not appear to affect the distribution of dissolved Al and Mn in the ACC in Drake Passage.

[46] Over the South American slope and near the Antarctic Peninsula, re-suspension of sedimentary particles and pore water influences the distribution of Al and Mn. The influence of these fluxes from the continental margins into Drake Passage was only visible near the continental slopes. On the Antarctic Peninsula side the Mn distribution was affected farther into the ACC than the Al distribution. However, with the perpendicular flow direction of the ACC through Drake Passage, the influence on the Al and Mn distribution downstream might be greater than can be concluded from this one section study. Higher [Al] observed eastward along the prime meridian might partly represent this effect in combination with accumulated dust input.

[47] Elevated [Al] and [Mn] were observed in the deepest part of Drake Passage due to sediment re-suspension from the deep Drake Passage sediments. In the deep southern Drake Passage, the elevated [Al] and [Mn] appears to be caused by sediment re-suspension during transport of the WSDW along the continental slope. From the north, NADW brings relatively high [Al] to the Drake Passage and this shows in elevated concentrations in LCDW. This influence is most profound in the northern most Drake Passage. Elevated [Mn] in the deep northern Drake Passage is related to the hydrothermal vent sources in the Pacific Ocean that the SPDSW passes on its journey to the Drake Passage.

[48] The vertical profile shape of both [Al] and [Mn] in Drake Passage is different from what is observed in other ocean basins, but more similar to the Atlantic section of the Southern Ocean. The [Al] reported in this study is lower than previously reported studies in or near Drake Passage, perhaps due to differences in sampling or analytical techniques. This issue stresses the importance of the use of both ultraclean sampling methods as well as standard reference water such as the GEOTRACES or SAFe standards. The [Mn] is comparable to previously reported profiles in the Drake Passage.

[49] **Acknowledgments.** This work was funded by the Netherlands Organisation for Scientific Research (NWO), IPY-NL-GEOTRACES sub-

project 851.40.101. The authors would like to express their gratitude to the master S. Schwarze and crew of R/V *Polarstern* for their unforgettable support during this expedition. Constructive comments of six reviewers and the associate editor are appreciated and have led to significant improvements of the manuscript. Special thanks to Loes Gerringa for her constructive comments and our colleagues Maarten Klunder and Charles-Edouard Thuróczy for their help with sampling and general support and to Sven Ober for the operation of the all-titanium CTD sampling system for trace metals. Sven Ober was assisted by Willem Polman who, together with the pilot, tragically lost his life during this expedition in a helicopter accident. His help and support were invaluable, as were his personality and presence. Willem Polman will therefore live on in our memories. After this tragic loss Michal Stimac stepped up to help with the operation of the TM sampling system. For this we are most grateful, as without his efforts we would not have been able to continue our work in the memory of the colleagues we lost. Finally, we would like to express a lot of gratitude to all participants of cruise ANT XXIV/3, for their help and support during this memorable expedition.

References

Aguilar-Islas, A., and K. W. Bruland (2006), Dissolved manganese and silicic acid in the Columbia River plume: A major source to the California Current and coastal waters off Washington and Oregon, *Mar. Chem.*, *101* (3–4), 223–247.

Baker, A. R., T. D. Jickells, M. Witt, and K. L. Linge (2006), Trends in the solubility of iron, aluminium, manganese and phosphorus in aerosol collected over the Atlantic Ocean, *Mar. Chem.*, *98*(1), 43–58, doi:10.1016/j.marchem.2005.06.004.

Baker, E. T., and C. R. German (2004), On the global distribution of hydrothermal vent fields, in *Mid-Ocean Ridges: Hydrothermal Interactions Between the Lithosphere and Oceans*, *Geophys. Monogr. Ser.*, vol. 148, edited by C. R. German, J. Lin, and L. M. Parson, pp. 245–266, AGU, Washington, D. C.

Barré, N., C. Provost, N. Sennechael, and J. H. Lee (2008), Circulation in the Ona Basin, southern Drake Passage, *J. Geophys. Res.*, *113*, C04033, doi:10.1029/2007JC004549.

Brown, M. T., and K. W. Bruland (2008), An improved flow-injection analysis method for the determination of dissolved aluminum in seawater, *Limnol. Oceanogr. Methods*, *6*, 87–95, doi:10.4319/lom.2008.6.87.

Brown, M. T., S. M. Lippiatt, and K. W. Bruland (2010), Dissolved aluminum, particulate aluminum, and silicic acid in northern Gulf of Alaska coastal waters: Glacial/riverine inputs and extreme reactivity, *Mar. Chem.*, *122*(1–4), 160–175, doi:10.1016/j.marchem.2010.04.002.

Bruland, K. W., and R. P. Franks (1983), Mn, Ni, Cu, Zn, and Cd in the western North Atlantic, in *Trace Metals in Sea Water*, edited by C. S. Wong et al., pp. 395–414, Plenum, New York.

Bruland, K. W., and M. C. Lohan (2004), The control of trace metals in seawater, in *The Oceans and Marine Geochemistry: Treatise on Geochemistry*, vol. 6, edited by H. D. Holland, and K. K. Turekian, pp. 23–47, Pergamon, Oxford, U. K.

Bruland, K. W., K. J. Orians, and J. P. Cowen (1994), Reactive trace metals in the stratified North Pacific, *Geochim. Cosmochim. Acta*, *58*(15), 3171–3182, doi:10.1016/0016-7037(94)90044-2.

Chou, L., and R. Wollast (1997), Biogeochemical behavior and mass balance of dissolved aluminum in the western Mediterranean Sea, *Deep Sea Res., Part II*, *44*(3–4), 741–768, doi:10.1016/S0967-0645(96)00092-6.

de Baar, H. J. W., et al. (2008), Titan: A new facility for ultraclean sampling of trace elements and isotopes in the deep oceans in the international Geotraces program, *Mar. Chem.*, *111*(1–2), 4–21, doi:10.1016/j.marchem.2007.07.009.

Doi, T., H. Obata, and M. Maruo (2004), Shipboard analysis of picomolar levels of manganese in seawater by chelating resin concentration and chemiluminescence detection, *Anal. Bioanal. Chem.*, *378*(5), 1288–1293, doi:10.1007/s00216-003-2483-z.

Elderfield, H. (1976), Manganese fluxes to the oceans, *Mar. Chem.*, *4*(2), 103–132, doi:10.1016/0304-4203(76)90001-3.

Farley, K. A., E. Maier-Reimer, P. Schlosser, and W. S. Broecker (1995), Constraints on mantle ^{3}He fluxes and deep-sea circulation from an oceanic general circulation model, *J. Geophys. Res.*, *100*(B3), 3829–3839, doi:10.1029/94JB02913.

Gehlen, M., L. Beck, G. Calas, A. M. Flank, A. J. Van Bennekom, and J. E. E. Van Beusekom (2002), Unraveling the atomic structure of biogenic silica: Evidence of the structural association of Al and Si in diatom frustules, *Geochim. Cosmochim. Acta*, *66*(9), 1601–1609, doi:10.1016/S0016-7037(01)00877-8.

Gehlen, M., C. Heinze, E. Maier-Reimer, and C. I. Measures (2003), Coupled Al-Si geochemistry in an ocean general circulation model: A tool for the validation of oceanic dust deposition fields?, *Global Biogeochem. Cycles*, *17*(1), 1028, doi:10.1029/2001GB001549.

Han, Q., J. K. Moore, C. Zender, C. Measures, and D. Hydes (2008), Constraining oceanic dust deposition using surface ocean dissolved Al, *Global Biogeochem. Cycles*, *22*, GB2003, doi:10.1029/2007GB002975.

Haraldsson, C., and S. Westerlund (1988), Trace metals in the water columns of the Black Sea and Framvaren Fjord, *Mar. Chem.*, *23*(3–4), 417–424, doi:10.1016/0304-4203(88)90108-9.

Heggie, D., G. Klinkhammer, and D. Cullen (1987), Manganese and copper fluxes from continental-margin sediments, *Geochim. Cosmochim. Acta*, *51*(5), 1059–1070, doi:10.1016/0016-7037(87)90200-6.

Hegner, E., H. J. Dauelsberg, M. M. R. van der Loeff, C. Jeandel, and H. J. W. de Baar (2007), Nd isotopic constraints on the origin of suspended particles in the Atlantic sector of the Southern Ocean, *Geochem. Geophys. Geosyst.*, *8*, Q10008, doi:10.1029/2007GC001666.

Hewes, C. D., C. S. Reiss, M. Kahru, B. G. Mitchell, and O. Holm-Hansen (2008), Control of phytoplankton biomass by dilution and mixed layer depth in the western Weddell-Scotia Confluence, *Mar. Ecol. Prog. Ser.*, *366*, 15–29, doi:10.3354/meps07515.

Hydes, D. J. (1977), Dissolved aluminium concentration in sea water, *Nature*, *268*(5616), 136–137, doi:10.1038/268136a0.

Hydes, D. J. (1979), Aluminum in seawater: Control by inorganic processes, *Science*, *205*(4412), 1260–1262, doi:10.1126/science.205.4412.1260.

Hydes, D. J., G. J. de Lange, and H. J. W. de Baar (1988), Dissolved aluminum in the Mediterranean, *Geochim. Cosmochim. Acta*, *52*(8), 2107–2114, doi:10.1016/0016-7037(88)90190-1.

Jacobs, L., S. Emerson, and S. S. Huested (1987), Trace metal geochemistry in the Cariaco Trench, *Deep-Sea Res.*, *34*(5–6), 965–981, doi:10.1016/0198-0149(87)90048-3.

Jickells, T. D., and J. D. Burton (1988), Cobalt, copper, manganese, and nickel in the Sargasso Sea, *Mar. Chem.*, *23*(1–2), 131–144, doi:10.1016/0304-4203(88)90027-8.

Johnson, K. S., W. M. Berelson, K. H. Coale, T. L. Coley, V. A. Elrod, W. R. Fairey, H. D. Iams, T. E. Kilgore, and J. L. Nowicki (1992), Manganese flux from continental margin sediments in a transect through the oxygen minimum, *Science*, *257*(5074), 1242–1245, doi:10.1126/science.257.5074.1242.

Johnson, K. S., et al. (2007), Developing standards for dissolved iron in seawater, *Eos Trans. AGU*, *88*(11), 131–132, doi:10.1029/2007EO110003.

Kaupp, L. J., C. I. Measures, K. E. Selph, and F. T. Mackenzie (2011), The distribution of dissolved Fe and Al in the upper waters of the Eastern Equatorial Pacific, *Deep Sea Res., Part II*, *58*(3–4), 296–310, doi:10.1016/j.dsr2.2010.08.009.

Klatt, O., E. Fahrbach, M. Hoppema, and G. Rohardt (2005), The transport of the Weddell Gyre across the Prime Meridian, *Deep Sea Res., Part II*, *52*(3–4), 513–528, doi:10.1016/j.dsr2.2004.12.015.

Klinkhammer, G. P., and M. L. Bender (1980), The distribution of manganese in the Pacific Ocean, *Earth Planet. Sci. Lett.*, *46*(3), 361–384, doi:10.1016/0012-821X(80)90051-5.

Klinkhammer, G. P., and A. Hudson (1986), Dispersal patterns for hydrothermal plumes in the South Pacific using manganese as a tracer, *Earth Planet. Sci. Lett.*, *79*(3–4), 241–249, doi:10.1016/0012-821X(86)90182-2.

Klinkhammer, G. P., M. L. Bender, and R. F. Weiss (1977), Hydrothermal manganese in the Galapagos rift, *Nature*, *269*(5626), 319–320, doi:10.1038/269319a0.

Klinkhammer, G. P., C. S. Chin, R. A. Keller, A. Dählmann, H. Sahling, G. Sarthou, S. Petersen, F. Smith, and C. Wilson (2001), Discovery of new hydrothermal vent sites in Bransfield Strait, Antarctica, *Earth Planet. Sci. Lett.*, *193*(3–4), 395–407, doi:10.1016/S0012-821X(01)00536-2.

Kramer, J., P. Laan, G. Sarthou, K. R. Timmermans, and H. J. W. de Baar (2004), Distribution of dissolved aluminium in the high atmospheric input region of the subtropical waters of the North Atlantic Ocean, *Mar. Chem.*, *88*(3–4), 85–101, doi:10.1016/j.marchem.2004.03.009.

Laës, A., S. Blain, P. Laan, S. J. Ussher, E. P. Achterberg, P. Treguer, and H. J. W. de Baar (2007), Sources and transport of dissolved iron and manganese along the continental margin of the Bay of Biscay, *Biogeosciences*, *4*(2), 181–194, doi:10.5194/bg-4-181-2007.

Landing, W. M., and K. W. Bruland (1980), Manganese in the North Pacific, *Earth Planet. Sci. Lett.*, *49*(1), 45–56, doi:10.1016/0012-821X(80)90149-1.

Landing, W. M., and K. W. Bruland (1987), The contrasting biogeochemistry of iron and manganese in the Pacific Ocean, *Geochim. Cosmochim. Acta*, *51*(1), 29–43, doi:10.1016/0016-7037(87)90004-4.

Landing, W. M., G. A. Cutter, J. A. Dalziel, A. R. Flegal, R. T. Powell, D. Schmidt, A. Shiller, P. Statham, S. Westerlund, and J. Resing (1995), Analytical intercomparison results from the 1990 Intergovernmental Oceanographic Commission open-ocean baseline survey for trace metals: Atlantic Ocean, *Mar. Chem.*, *49*(4), 253–265, doi:10.1016/0304-4203(95)00016-K.

Lenn, Y. D., T. K. Chereskin, and J. Sprintall (2008), Improving estimates of the Antarctic Circumpolar Current streamlines in Drake Passage, *J. Phys. Oceanogr.*, *38*, 1000–1010, doi:10.1175/2007JPO3834.1.

Lewis, B. L., and W. M. Landing (1991), The biogeochemistry of manganese and iron in the Black Sea, *Deep Sea Res.*, *38*, suppl. 1.2, 773–803.

Li, F., P. Ginoux, and V. Ramaswamy (2008), Distribution, transport, and deposition of mineral dust in the Southern Ocean and Antarctica: Contribution of major sources, *J. Geophys. Res.*, *113*, D10207, doi:10.1029/2007JD009190.

Mackin, J. E., and R. C. Aller (1984a), Processes affecting the behavior of dissolved aluminum in estuarine waters, *Mar. Chem.*, *14*(3), 213–232, doi:10.1016/0304-4203(84)90043-4.

Mackin, J. E., and R. C. Aller (1984b), Diagenesis of dissolved aluminum in organic-rich estuarine sediments, *Geochim. Cosmochim. Acta*, *48*(2), 299–313, doi:10.1016/0016-7037(84)90252-7.

Mackin, J. E., and R. C. Aller (1986), The effects of clay mineral reactions on dissolved Al distributions in sediments and waters of the Amazon continental shelf, *Cont. Shelf Res.*, *6*(1–2), 245–262, doi:10.1016/0278-4343(86)90063-4.

Martin, J. H., R. M. Gordon, and S. E. Fitzwater (1990), Iron in Antarctic waters, *Nature*, *345*(6271), 156–158, doi:10.1038/345156a0.

Measures, C. I. (1999), The role of entrained sediments in sea ice in the distribution of aluminium and iron in the surface waters of the Arctic Ocean, *Mar. Chem.*, *68*(1–2), 59–70, doi:10.1016/S0304-4203(99)00065-1.

Measures, C. I., and E. T. Brown (1996), Estimating dust input to the Atlantic Ocean using surface water Al concentrations, in *The Impact of Desert Dust Across the Mediterranean*, edited by S. Guerzoni and R. Chester, pp. 301–311, Kluwer, Dordrecht, Netherlands.

Measures, C. I., and J. M. Edmond (1990), Aluminium in the South Atlantic: Steady state distribution of a short residence element, *J. Geophys. Res.*, *95*(C4), 5331–5340, doi:10.1029/JC095iC04p05331.

Measures, C. I., and J. M. Edmond (1992), The distribution of aluminium in the Greenland Sea and its relationship to ventilation processes, *J. Geophys. Res.*, *97*(C11), 17,787–17,800, doi:10.1029/92JC01798.

Measures, C. I., and S. Vink (2000), On the use of dissolved aluminum in surface waters to estimate dust deposition to the ocean, *Global Biogeochem. Cycles*, *14*(1), 317–327, doi:10.1029/1999GB001188.

Measures, C. I., M. T. Brown, and S. Vink (2005), Dust deposition to the surface waters of the western and central North Pacific inferred from surface water dissolved aluminum concentrations, *Geochem. Geophys. Geosyst.*, *6*, Q09M03, doi:10.1029/2005GC000922.

Middag, R. (2010), Dissolved aluminium and manganese in the polar oceans, PhD thesis, Univ. of Groningen, Groningen, Netherlands.

Middag, R., H. J. W. de Baar, P. Laan, and K. Bakker (2009), Dissolved aluminium and the silicon cycle in the Arctic Ocean, *Mar. Chem.*, *115*(3–4), 176–195, doi:10.1016/j.marchem.2009.08.002.

Middag, R., C. Van Slooten, H. J. W. de Baar, and P. Laan (2011a), Dissolved aluminium in the Southern Ocean, *Deep Sea Res., Part II*, *58*(25–26), 2647–2660, doi:10.1016/j.dsr2.2011.03.001.

Middag, R., H. J. W. de Baar, P. Laan, and M. B. Klunder (2011b), Fluvial and hydrothermal input of manganese into the Arctic Ocean, *Geochim. Cosmochim. Acta*, *75*(9), 2393–2408, doi:10.1016/j.gca.2011.02.011.

Middag, R., H. J. W. de Baar, P. Laan, P. H. Cai, and J. Van Ooijen (2011c), Dissolved manganese in the Atlantic section of the Southern Ocean, *Deep Sea Res., Part II*, *58*(25–26), 2661–2677, doi:10.1016/j.dsr2.2010.10.043.

Moore, R. M., and G. E. Millward (1984), Dissolved-particulate interactions of aluminium in ocean water, *Geochim. Cosmochim. Acta*, *48*(2), 235–241, doi:10.1016/0016-7037(84)90247-3.

Moran, S. B., and R. M. Moore (1992), Kinetics of the removal of dissolved aluminum by diatoms in seawater: A comparison with thorium, *Geochim. Cosmochim. Acta*, *56*(9), 3365–3374, doi:10.1016/0016-7037(92)90384-U.

Morley, N. H., P. J. Statham, and J. D. Burton (1993), Dissolved trace metals in the southwestern Indian Ocean, *Deep Sea Res., Part I*, *40*(5), 1043–1062, doi:10.1016/0967-0637(93)90089-L.

Orians, K. J., and K. W. Bruland (1985), Dissolved aluminum in the central North Pacific, *Nature*, *316*(6027), 427–429, doi:10.1038/316427a0.

Orians, K. J., and K. W. Bruland (1986), The biogeochemistry of aluminum in the Pacific Ocean, *Earth Planet. Sci. Lett.*, *78*(4), 397–410, doi:10.1016/0012-821X(86)90006-3.

Orians, K. J., and K. W. Bruland (1988), The marine geochemistry of dissolved gallium: A comparison with dissolved aluminum, *Geochim. Cosmochim. Acta*, *52*(12), 2955–2962, doi:10.1016/0016-7037(88)90160-3.

Pakhomova, S. V., P. O. J. Hall, M. Y. Kononets, A. G. Rozanov, A. Tengberg, and A. V. Vershinin (2007), Fluxes of iron and manganese across the sediment-water interface under various redox conditions, *Mar. Chem.*, *107*(3), 319–331, doi:10.1016/j.marchem.2007.06.001.

Percy, D., X. N. Li, G. T. Taylor, Y. Astor, and M. I. Scranton (2008), Controls on iron, manganese and intermediate oxidation state sulfur compounds in the Cariaco Basin, *Mar. Chem.*, *111*(1–2), 47–62, doi:10.1016/j.marchem.2007.02.001.

Pollard, R. T., M. I. Lucas, and J. F. Read (2002), Physical controls on biogeochemical zonation in the Southern Ocean, *Deep Sea Res., Part II*, *49*, 3289–3305, doi:10.1016/S0967-0645(02)00084-X.

Rutgers van der Loeff, M. M., P. S. Meadows, and J. A. Allen (1990), Oxygen in pore waters of deep-sea sediments, *Philos. Trans. R. Soc. A*, *331*(1616), 69–84, doi:10.1098/rsta.1990.0057.

Rutgers van der Loeff, M. M., P. H. Cai, I. Stimac, R. Middag, M. B. Klunder, and S. Van Heuven (2011), ^{234}Th in surface waters: Distribution of particle export flux across the Antarctic Circumpolar Current and in the Weddell Sea during the GEOTRACES expedition ZERO and DRAKE, *Deep Sea Res., Part II*, *58*(25–26), 2749–2766, doi:10.1016/j.dsr2.2011.02.004.

Saager, P. M., H. J. W. de Baar, and P. H. Burkill (1989), Manganese and iron in Indian Ocean waters, *Geochim. Cosmochim. Acta*, *53*(9), 2259–2267, doi:10.1016/0016-7037(89)90348-7.

Saager, P. M., H. J. W. de Baar, J. T. M. de Jong, R. F. Nolting, and J. Schijf (1997), Hydrography and local sources of dissolved Mn, Ni, Cu and Cd in the northeast Atlantic Ocean, *Mar. Chem.*, *57*(3–4), 195–216, doi:10.1016/S0304-4203(97)00038-8.

Sedwick, P. N., P. R. Edwards, D. J. Mackey, F. B. Griffiths, and J. S. Parslow (1997), Iron and manganese in surface waters of the Australian subantarctic region, *Deep Sea Res., Part I*, *44*(7), 1239–1253, doi:10.1016/S0967-0637(97)00021-6.

Sedwick, P. N., G. R. DiTullio, and D. J. Mackey (2000), Iron and manganese in the Ross Sea, Antarctica: Seasonal iron limitation in Antarctic shelf waters, *J. Geophys. Res.*, *105*(C5), 11,321–11,336, doi:10.1029/2000JC000256.

Shiller, A. M. (1997), Manganese in surface waters of the Atlantic Ocean, *Geophys. Res. Lett.*, *24*(12), 1495–1498, doi:10.1029/97GL01456.

Statham, P. J., P. A. Yeats, and W. M. Landing (1998), Manganese in the eastern Atlantic Ocean: Processes influencing deep and surface water distributions, *Mar. Chem.*, *61*(1–2), 55–68, doi:10.1016/S0304-4203(98)00007-3.

Stoffyn, M. (1979), Biological control of aluminum in seawater: Experimental evidence, *Science*, *203*(4381), 651–653, doi:10.1126/science.203.4381.651.

Stoffyn, M., and F. T. Mackenzie (1982), Fate of dissolved aluminum in the oceans, *Mar. Chem.*, *11*(2), 105–127, doi:10.1016/0304-4203(82)90036-6.

Sudre, J., V. Garcon, C. Provost, N. Sennéchael, O. Huhn, and M. Lacombe (2011), Short-term variations of deep water masses in Drake Passage revealed by a multiparametric analysis of the ANT-XXIII/3 bottle data, *Deep Sea Res., Part II*, *58*(25–26), 2592–2612, doi:10.1016/j.dsr2.2011.01.005.

Sültenfuß, J., M. Rhein, and W. Roether (2009), The Bremen Mass Spectrometric Facility for the measurement of helium isotopes, neon, and tritium in water, *Isotopes Environ. Health Stud.*, *45*(2), 1–13.

Sunda, W. G., and S. A. Huntsman (1988), Effect of sunlight on redox cycles of manganese in the southwestern Sargasso Sea, *Deep Sea Res., Part A*, *35*(8), 1297–1317, doi:10.1016/0198-0149(88)90084-2.

Sunda, W. G., and S. A. Huntsman (1994), Photoreduction of manganese oxides in seawater, *Mar. Chem.*, *46*(1–2), 133–152, doi:10.1016/0304-4203(94)90051-5.

Sunda, W. G., S. A. Huntsman, and G. R. Harvey (1983), Photoreduction of manganese oxides in seawater and its geochemical and biological implications, *Nature*, *301*(5897), 234–236, doi:10.1038/301234a0.

Sundby, B., and N. Silverberg (1985), Manganese fluxes in the benthic boundary layer, *Limnol. Oceanogr.*, *30*(2), 372–381, doi:10.4319/lo.1985.30.2.0372.

Tebo, B. M., B. G. Clement, and G. J. Dick (2007), Biotransformations of manganese, in *Manual of Environmental Microbiology*, 3rd ed., edited by C. J. Hurst et al., pp. 1223–1238, ASM Press, Washington, D. C.

Tria, J., E. C. V. Butler, P. R. Haddad, and A. R. Bowie (2007), Determination of aluminium in natural water samples, *Anal. Chim. Acta*, *588*(2), 153–165, doi:10.1016/j.aca.2007.02.048.

Van Bennekom, A. J., A. G. J. Buma, and R. F. Nolting (1991), Dissolved aluminium in the Weddell-Scotia Confluence and effect of Al on the dissolution kinetics of biogenic silica, *Mar. Chem.*, *35*(1–4), 423–434, doi:10.1016/S0304-4203(09)90034-2.

Van Beueskom, J. E. E., A. J. van Bennekom, P. Tréguer, and J. Morvan (1997), Aluminium and silicic acid in water and sediments of the Enderby and Crozet Basins, *Deep Sea Res., Part II*, *44*(5), 987–1003, doi:10.1016/S0967-0645(96)00105-1.

Wedepohl, K. H. (1995), The composition of the continental crust, *Geochim. Cosmochim. Acta*, *59*(7), 1217–1232, doi:10.1016/0016-7037(95)00038-2.

Well, R., W. Roether, and D. P. Stevens (2003), An additional deep-water mass in Drake Passage as revealed by ^{3}He data, *Deep Sea Res., Part I*, *50*, 1079–1098, doi:10.1016/S0967-0637(03)00050-5.

Westerlund, S., and P. Öhman (1991), Iron in the water column of the Weddell Sea, *Mar. Chem.*, *35*(1–4), 199–217, doi:10.1016/S0304-4203(09)90018-4.

Whitworth, T., and W. D. Nowlin (1987), Water masses and currents of the Southern Ocean at the Greenwich Meridian, *J. Geophys. Res.*, *92*, 6462–6476, doi:10.1029/JC092iC06p06462.

Yeats, P. A. (1988), Manganese, nickel, zinc and cadmium distributions at the Fram 3 and Cesar ice camps in the Arctic Ocean, *Oceanol. Acta*, *11*(4), 383–388.

Yemenicioglu, S., S. Erdogan, and S. Tagrul (2006), Distribution of dissolved forms of iron and manganese in the Black Sea, *Deep Sea Res., Part II*, *53*(17–19), 1842–1855, doi:10.1016/j.dsr2.2006.03.014.

H. J. W. de Baar, P. Laan, and R. Middag, Royal Netherlands Institute for Sea Research, Landsdiep 4, Den Burg NL-1797 SZ, Texel, Netherlands. (rob.middag@nioz.nl)

O. Huhn, Institut für Umweltphysik, Universität Bremen, Otto-Hahn-Allee, Bremen D-28359, Germany.